IEEE Access
Multidisciplinary | Rapid Review | Open Access Journal

Received July 8, 2020, accepted July 12, 2020, date of publication July 22, 2020, date of current version August 5, 2020.

Digital Object Identifier 10.1109/ACCESS.2020.3011364

Post-Mortem Iris Recognition–A Survey and Assessment of the State of the Art

AIDAN BOYD[1], (Student Member, IEEE), SHIVANGI YADAV[2], THOMAS SWEARINGEN[2], (Student Member, IEEE), ANDREY KUEHLKAMP[1], (Member, IEEE), MATEUSZ TROKIELEWICZ[3], (Member, IEEE), ERIC BENJAMIN[4], PIOTR MACIEJEWICZ[5], DENNIS CHUTE[4], ARUN ROSS[2], (Senior Member, IEEE), PATRICK FLYNN[1], (Fellow, IEEE), KEVIN BOWYER[1], (Fellow, IEEE), AND ADAM CZAJKA[1], (Senior Member, IEEE)

[1]Computer Science and Engineering, University of Notre Dame, Notre Dame, IN 46656, USA
[2]Computer Science and Engineering, Michigan State University, East Lansing, MI 48824, USA
[3]NASK National Research Institute, 01-045 Warsaw, Poland
[4]Dutchess County Medical Examiner Office, Poughkeepsie, NY 12601, USA
[5]Department of Ophthalmology, Medical University of Warsaw, 01-045 Warsaw, Poland

Corresponding author: Aidan Boyd (aboyd3@nd.edu)

This work was supported by the National Institute of Justice, Office of Justice Programs, U.S. Department of Justice, under Award 2018-DU-BX-0215. The opinions, findings, and conclusions or recommendations expressed in this publication are those of the authors and do not necessarily reflect those of the Department of Justice.

ABSTRACT Post-mortem biometrics entails utilizing the biometric data of a deceased individual for determining or verifying human identity. Due to fundamental biological changes that occur in a person's biometric traits after death, post-mortem data can be significantly different from ante-mortem data, introducing new challenges for biometric sensors, feature extractors and matchers. This paper surveys research to date on the problem of using iris images acquired after death for automated human recognition. A comprehensive review of existing literature is complemented by a summary of the most recent results and observations offered in these publications. This survey is unique in several elements. Firstly, it is the first publication to consider iris recognition where gallery images are acquired before death (peri-mortem images) and the probe images are acquired after death from the same subjects. Secondly, results are presented from the largest database of peri-mortem and post-mortem iris images, collected from 213 subjects by two independent institutions located in the U.S. and Poland. Thirdly, post-mortem recognition viability is assessed using more than 20 iris recognition algorithms, ranging from the classic (e.g., Gabor filtering-based) to the modern (e.g., deep learning-based). Finally, we provide a medically informed commentary on post-mortem iris, analyze the reasons for recognition failures, and identify key directions for future research.

INDEX TERMS Forensics, iris recognition, post-mortem biometrics.

I. INTRODUCTION

Biometrics is the science of recognizing individuals based on their biological and behavioral characteristics such as fingerprints, face, iris, voice, and gait [1]. A typical biometric system employs a sensor to capture a sample of the biometric attribute of an individual, extracts features from the acquired biometric sample, and compares the features extracted from two biometric samples to generate a match score. Based on the match score, a decision is rendered as to whether the two biometric samples originate from the same source or from two different sources. While a number of biometric traits have been proposed in the literature, the face, fingerprint, voice and iris modalities have been extensively studied and deployed in a number of applications [2]. In this work we focus on the iris modality.

Iris recognition entails comparing the texture of the iris present in ocular images. The human iris is an internal organ of the eye that controls the pupil size in response to the amount of light reaching the retina. It is a colored ring-shaped region with the pupillary boundary as the inner border and the ciliary boundary as the outer border, as shown in Figure 2. The texture of the iris region is the important source of features used for recognition. The detailed texture pattern

The associate editor coordinating the review of this manuscript and approving it for publication was Derek Abbott.

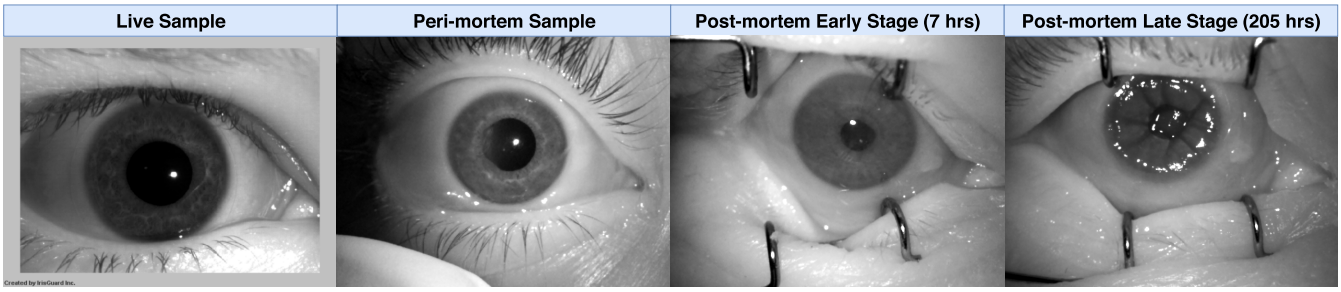

FIGURE 1. Four different iris types considered in this survey: the live sample (acquired before death), peri-mortem sample (acquired around the time of death) and post-mortem samples (acquired after death). The two post-mortem samples are from the same subject, while the live and peri-mortem samples are from different subjects. These samples illustrate changes in iris appearance over time. They were acquired in near-infrared light (centered around 810 nm) by an iris sensor that produces iris images compliant with the ISO/IEC 19794-6 standard.

is highly specific to the particular individual iris. From the perspective of traditional iris recognition algorithms, the two irides of the same person, or two irides of monozygotic twins, are as different as irides of unrelated persons. The iris is well protected by the cornea, yet easily imaged through it. These properties combine to make the iris very attractive as a biometric identifier. As is the case with every biometric mode, there is ongoing research related to various challenges, including such things as presentation attack detection, dealing with eye diseases, application to identification of newborns, understanding aging processes and developing algorithms that are agnostic to age-related changes, and assessing reliability of post-mortem iris recognition [3].

The belief that the iris decays 'soon' after death in a way that makes iris recognition impossible has pervaded iris recognition research since its beginning. This belief was often used to neutralize gruesome, yet mythical, scenarios of presenting eyeballs plucked from the eye socket to iris scanners. However, recent studies demonstrate that the dynamics of eye and iris decomposition, from the biometric point of view, are more complex and less rapid than initially believed. These processes heavily depend on the ambient conditions, but today we know that iris patterns can still be useful for recognition a few days after death in a warm environment [4], [5], or up to even a few weeks in a mortuary environment [6]–[8].

Examples of different types of iris images considered in this work are shown in Figure 1. From this it can be deduced that for the live and peri-mortem irides, the distinctive features and textural patterns of the iris are apparent. However, in the time between the early post-mortem stage and the late post-mortem stage, we see deformations of the cornea and, possibly, the iris texture that make extraction of iris features less reliable. This paper investigates the effect of this degradation in relation to the task of iris recognition.

Although this survey is focused on iris, the face and fingerprint modalities also offer potential postmortem biometric recognition utility. Some preliminary studies [4], [5] on automated recognition for postmortem face and fingerprint explored the length-of-viability of the trait when left exposed to the natural elements. This of course varies with temperature, humidity and season.

There would be no contemporary medicine without the study and understanding of the human body. Most of our basic anatomical knowledge, contributing later to development of advanced surgery, has been gained from cadavers. Such research activities require an ethical and moral respect for the human body and the acknowledgment of the generosity of relatives of the deceased. It is in this spirit that a unique post-mortem iris recognition study is being conducted by five institutions (Medical University of Warsaw, NASK National Research Institute, University of Notre Dame, Dutchess County Medical Examiner's Office and Michigan State University). We hope that this survey can serve as a source of accurate technical knowledge for those who wish to understand the advances and challenges in post-mortem iris recognition. The specific contributions of this survey include:

- a unique study in which iris images acquired before death (peri-mortem) and after death (post-mortem) from the same subjects are compared;
- an assessment of post-mortem iris recognition accuracy based on over 20 iris recognition methods, including classic (Gabor filtering-based) and modern (deep learning-based) approaches, on a database of 213 subjects, which is the largest such database to date;
- a medical commentary related to post-mortem iris recognition;
- an explanation of reasons for recognition failures, along with suggestions for future research directions that could address these issues.

II. APPLICATION SCENARIOS

Post-mortem iris recognition is useful in typical forensic scenarios, where ante-mortem data has to be matched with information gathered from deceased subjects in order to obtain a list of potential matching identities. For short time horizons (not exceeding three weeks [8]) and favorable conditions (*e.g.*, cadavers kept in low temperatures), iris recognition is already known to offer superior speed over other

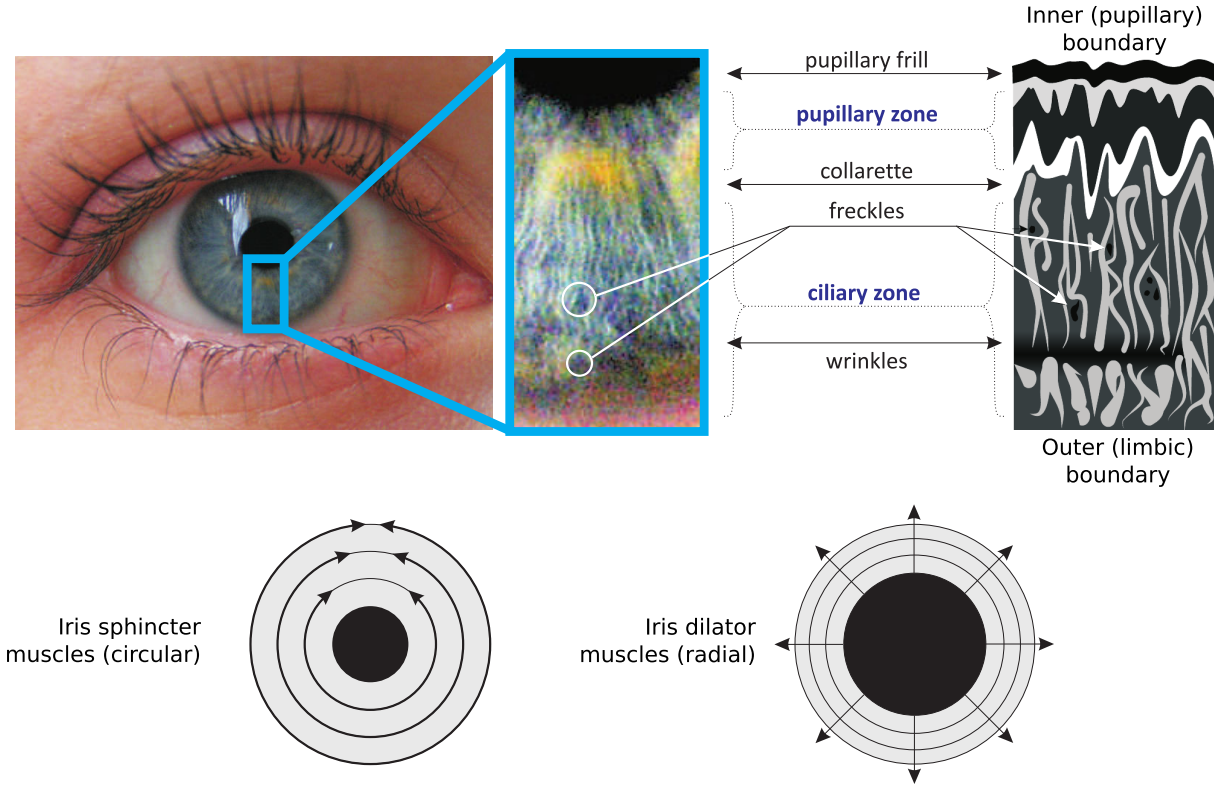

FIGURE 2. The iris pattern is a very rich structure composed of various elements, such as ciliary processes, Fuchs' crypts (anterior surface openings, usually located near the collarette and surrounded by collagen trabeculae), Krückmann-Wolfflin bodies (stromal condensations, especially in blue or hazel eyes), freckles (local concentrations of melanin pigment), and contraction folds as a consequence of iris dilation and constriction (owing to the dilator and sphincter muscles).

well-established forensic identification tools, such as DNA or dental records. Under the same temporal and environmental assumptions, iris recognition should offer substantially higher accuracy than ''soft biometrics'' methods, such as sex, age, ethnicity, or eye/skin/hair color.

In addition to the short-term time horizon and appropriate conditions of cadaver storage, the forensic scenario requires iris samples collected before death to match against. Although iris recognition is slowly becoming ubiquitous, mainly due to various governmental programs (*e.g.*, NEXUS/CANPASS at the US/Canada border [9], AADHAAR in India [10], voter registration in Ghana, Tanzania and Somaliland [11], and biometric passports), it is not as common as face imaging, which is widely used for many identity documents. Thus, ante-mortem vs post-mortem iris matching is likely to remain as a niche forensic technique for the foreseeable future. However, specific deployments of iris recognition, such as 'iris at a distance' [12] or cross-wavelength (near-infrared vs visible light) iris matching [13]–[15], may increase its importance and result in iris templates being used more frequently in various identification efforts.

There is, however, another important scenario, which does not incorporate ante-mortem data: rapid registration of bodies found at mass fatality incidents to be later tracked and dispatched appropriately to correct destinations. If cadavers need to be tracked for short time periods (as mentioned above, up to a few weeks), and the iris pattern of at least one eye is visible, then iris recognition seems to offer a useful alternative in such situations.

III. APPLICATION SCENARIOS

Post-mortem iris recognition is useful in typical forensic scenarios, where ante-mortem data has to be matched with information gathered from deceased subjects in order to obtain a list of potential matching identities. For short time horizons (not exceeding three weeks [8]) and favorable conditions (*e.g.*, cadavers kept in low temperatures), iris recognition is already known to offer superior speed over other well-established forensic identification tools, such as DNA or dental records. Under the same temporal and environmental assumptions, iris recognition should offer substantially higher accuracy than ''soft biometrics'' methods, such as sex, age, ethnicity, or eye/skin/hair color.

In addition to the short-term time horizon and appropriate conditions of cadaver storage, the forensic scenario requires iris samples collected before death to match against. Although iris recognition is slowly becoming ubiquitous, mainly due to various governmental programs (*e.g.*, NEXUS/CANPASS at the US/Canada border [9], AADHAAR in India [10], voter registration in Ghana, Tanzania and Somaliland [11], and biometric passports), it is

not as common as face imaging, which is widely used for many identity documents. Thus, ante-mortem vs post-mortem iris matching is likely to remain as a niche forensic technique for the foreseeable future. However, specific deployments of iris recognition, such as 'iris at a distance' [12] or cross-wavelength (near-infrared vs visible light) iris matching [13]–[15], may increase its importance and result in iris templates being used more frequently in various identification efforts.

There is, however, another important scenario, which does not incorporate ante-mortem data: rapid registration of bodies found at mass fatality incidents to be later tracked and dispatched appropriately to correct destinations. If cadavers need to be tracked for short time periods (as mentioned above, up to a few weeks), and the iris pattern of at least one eye is visible, then iris recognition seems to offer a useful alternative in such situations.

IV. POST-MORTEM DECOMPOSITION OF AN EYE FROM THE MEDICAL SCIENCE STANDPOINT

Postmortem study of the eye globes has been of interest to forensic sciences for several years as a means to assist with the estimation of the postmortem interval [16]–[20]. Various chemical and physical postmortem changes of the eyes have been investigated in human and animal studies [21]. These include vitreous chemistry, such as electrolytes (sodium, potassium, etc.), as well as postmortem assays for alcohol and drugs (drugs of abuse and prescription medications) [22]. Postmortem examination of different components of the eye are studied, such as corneal thickness, corneal clouding, changes in pupillary diameter, changes in tonicity of the globes, and changes to the retinal vessels and neurologic tissue [23]–[29]. In particular, pupils are usually mid-dilated after death, in the so-called *cadaveric position*, which *de facto* makes the automatic post-mortem iris recognition easier: with pupils being neither heavily dilated nor heavily constricted, the iris textural features are well visible and not deformed, and the post-mortem dilation is constant.

Little is written about postmortem iris musculature per se, although studies have been done on pupil diameter changes by applying mydriatic and miotic agents. Research into the persistent ability of skeletal muscle to contract postmortem has also been done, but not on the iris directly. However, it seems reasonable to expect that these postmortem features may apply to iris muscles as well [30]–[32], and thus to assume that within the first couple of hours after death, the iris may react to pupillomotoric drugs; e.g., pilocarpine and atropine. Because the iris does not react to light after death, pupil dynamics-based liveness detection is straightforward, and post-mortem eyes are easily detected by systems implementing this approach to presentation attack detection.

Another factor to consider is whether irides change color postmortem as suggested by some forensic textbooks [33], [34]. A recent porcine study indicated that irides do darken in color within 48-72 hours after death, although comparable human studies have not been published [35]. In the study by Abraham *et al.*, porcine globes were placed in different controlled temperature environments and observed for color changes to irides. All globes placed in a 30-36°C temperature oven desiccated, hardened and turned dark by 36 hours. Globes placed in a 25°C isothermal environment were desiccated and darkened by 48 hours. Those globes placed in a 6°C environment showed persistence of iris color up to 60 hours. The porcine globes, like human globes, also demonstrated a well-known postmortem artifact called *tache noire*. In humans this is recognized as a band-like darkening of the sclera subsequent to desiccation. *Tache noire* may develop when the eyelids are left separated postmortem; on occasion it may affect the sclera more diffusely, so-called, *global tache noire* [36]. Also, due to reduced intraocular pressure, the globe depresses usually in the central part and loses its firmness [27].

V. REVIEW OF POST-MORTEM IRIS RECOGNITION EFFORTS TO DATE

A. PAPERS STUDYING THE FEASIBILITY OF POST-MORTEM IRIS BIOMETRICS

Probably the first researcher to approach the problem of iris recognition after death was Sansola, who focused on authenticating human subjects after death using iris recognition [37]. With an IriShield M2120U iris sensor and IriCore software, she enrolled 43 subjects who had their irides photographed at different post-mortem time horizons. Depending on the post-mortem interval, the method yielded 19-30% false non-matches and no false matches. Sansola also reported a relationship between the eye color and post-mortem comparison scores, with blue/gray eyes yielding lower correct match rates (59%) than brown (82%) or green/hazel eyes (88%).

Because of the obvious difficulty of organizing a human post-mortem data collection protocol, some researchers turned to experiments involving animals. A study involving domestic pigs was conducted by Saripalle *et al.*, who concluded that irides degrade slowly after being taken out of the body, and lose their biometric capabilities 6 to 8 hours after death [38].

Trokielewicz *et al.* showed that the iris can still successfully serve as a biometric identifier for 27 hours after death [6]. Images were collected in three acquisition sessions: session 1, 5-7 hours post-mortem; session 2, 16.5-21 hours post-mortem; and session 3: 27 hours post-mortem. They were able to show that irides can be encoded and recognized in more than 90% of the session 1 cases. Effects of iris degradation where observed in session 2, with FNMR increasing significantly to 48.88% for the OSIRIS method. However, two commercial matchers – IriTech and MIRLIN – still present fairly good ability to recognize the samples; approx. 94.96% and 82.76% correct verifications, respectively. In session 3, 73.33% of irides were still correctly recognized 27 hours after death using the IriCore method, whereas the performance of the remaining methods was uneven, as they were able to recognize from 13.33% (OSIRIS) to 60% (VeriEye).

Trokielewicz *et al.* extended their experiments, introducing a larger database with samples collected up to 17 days post-mortem [7]. A short-term analysis, concentrating on samples acquired up to 60 hours after death, revealed that the best performing IriCore method can still offer EER as low as 13%, which indicates that iris recognition can still be a reasonable identification tool after such a period of time. Long-term analysis taking into account all samples collected over a period of 17 days, however, shows that the iris deterioration progresses substantially over this longer time horizon, and although correct matches can still occur even after 17 days, they are sparse and cannot be considered as a reliable proof of one's identity.

Bolme *et al.* [4] tracked biometric capabilities of face, fingerprint and iris during human decomposition in outdoor conditions. Twelve subjects were placed in a body farm to assess how the environment and time affect performance of biometric methods. Although fingerprints and face were shown to be moderately resilient to decomposition, the irides degraded quickly regardless of the temperature. Irides typically became useless from the recognition viewpoint only a few days after exposition to outdoor conditions, and if the bodies were kept outside for 14 days the correct verification rate was near zero. A follow-up paper by Sauerwein *et al.* [5] showed that irides stay readable for up to 34 days after death, when cadavers were kept in outdoor conditions during winter. The readability was assessed by human experts acquiring the samples and no iris recognition algorithms were used in this study, however these observations suggest that low temperatures increase the chances to see an iris even in a cadaver left outside for a longer time.

Trokielewicz *et al.* [8] recently further extended the database of cadaver iris samples collected at the Medical University of Warsaw, Warsaw University of Technology, and NASK – National Research Institute. The study showed that correct matches are possible for even as long as 21 days after death, pinpointed segmentation errors as the most prominent source of recognition failures, and assessed the chances of false matches when post-mortem iris samples are compared against databases of live iris samples.

Branching out from the field of biometrics and into the field of forensic and legal medicine, a recent paper by Trokielewicz *et al.* gives insight into the decomposition processes taking place in the human eye after death from the perspective of automatic identity recognition [39]. The authors argue that such applications may prove useful *"for fast and accurate matching of ante-mortem with post-mortem data acquired at crime scenes or mass casualties, as well as for ensuring correct dispatching of bodies from the incident scene to a mortuary or funeral homes"*. The paper provides an analysis of global and local changes during the eyeball decay of one subject, and itemizes possible guidelines for forensic examiners employing iris biometrics during their proceedings.

B. PAPERS PROPOSING POST-MORTEM-SPECIFIC IRIS RECOGNITION METHODOLOGIES

Trokielewicz and Czajka [40] proposed a method for segmenting iris images from deceased subjects. By training a deep convolutional encoder-decoder with more than 1,300 manually-annotated occlusion masks, they obtained consistent and accurate predictions for iris regions in post-mortem iris samples. They open-sourced both the binary iris masks used for training, as well as the weights of the trained model.

Trokielewicz *et al.* showed that a reliable presentation attack detection method can be constructed to detect cadaver iris presentations [41], reaching 99% accuracy. This allowed to build a system with APCER=0 %@BPCER=1% (Attack Presentation and Bona Fide Presentation Classification Error Rates, respectively) for samples collected at least 16 hours post-mortem. Countermeasures to minimize the bias caused by image properties that are not related to PAD are implemented, and analysis of class activation maps to ensure that discriminant iris regions utilized by the classifier were related to properties of the eye, and not of the specific acquisition protocol.

Cadaver-focused iris image segmentation proposed in [40] was extended by Trokielewicz *et al.*, using two different, convolutional neural network-based segmentation models trained on a variety of iris image datasets, including post-mortem data [42], [43]. One model is suited for detecting the rough iris and sclera boundaries, whereas the second yields predictions of iris regions unaffected by post-mortem tissue decomposition. This work also shows how to normalize irregular segmentation masks provided by neural networks for use in a Gabor-based iris recognition pipeline, which gave an improvement in recognition accuracy over the methods designed only for ante-mortem irises.

Trokielewicz proposed the first post-mortem-specific iris feature representation, which employed Siamese networks to learn filter kernels that would accurately describe iris features altered by post-mortem decay processes [44], [45]. A hybrid filter bank is proposed, comprising a mixture of Gabor and Siamese-learnt kernels. Such an approach allowed for reduced error rates for all post-mortem intervals explored – from 12 hours to 369 hours post-mortem – compared to a state-of-the-art commercial iris matching technology (IriCore).

Exploring the concept of post-mortem iris recognition as a useful tool for forensic proceedings, Trokielewicz *et al.* studied the differences in perceiving iris features by both human examiners tasked with iris verification, as well as by a convolutional neural network-based classifier. This was done by recording the gaze of humans during iris examination and comparing their fixation points against saliency maps obtained from the machine solution. Conclusions include that the machine classifier can provide complementary cues regarding matching or non-matching regions, since the saliency maps provided by humans and by machines rarely overlap. Another observation is that both humans and

TABLE 1. Summary of the research literature on post-mortem iris recognition. Acronyms used in the table: FNMR: False Non-Match Rate; FMR: False Match Rate; EER: Equal Error Rate; CNN: Convolutional Neural Network; NIR: Near Infrared; PAD: Presentation Attack Detection.

Authors	Year	Number of subjects	Main findings	New database offered	Source codes or models available
Sansola [37]	2015	43	FNMR from 19% to 30% reported for post-mortem iris samples depending on the time since death.	No	No
Saripalle *et al.* [38]	2015	17 eyes	Ex-vivo pig eyes lose biometric capabilities approx. 8 hours after being taken out of the cadaver.	No	No
Trokielewicz *et al.* [6]	2016	17	Post-mortem iris verification can work up to 27 hours after death; no excessive pupil dilation observed. (FNMR=26.7% for the IriCore method, 27 hours since death)	No	No
Trokielewicz *et al.* [7]	2016	17	EER=13% up to 60 hours post-mortem for the IriCore method; occasional matches up to 17 days, but iris tissue deterioration was extensive.	Yes (17 subjects)	No
Bolme *et al.* [4]	2016	12	Correct verification rate 0.6% for bodies kept outdoor for 14 days (assessment by automatic methods).	No	No
Sauerwein *et al.* [5]	2017	12	Some irides readable after 34 days outdoor during winter (assessment by a human examiner).	No	No
Trokielewicz *et al.* [8]	2018	37	Occasional correct matches up to 21 days post-mortem; comparing post-mortem samples to live samples can yield increased FMRs.	Yes (20 subjects)	No
Trokielewicz *et al.* [40]	2018	37	CNN-based post-mortem-aware iris image segmentation proposed.	No	Yes (CNN model weights)
Trokielewicz *et al.* [41]	2018	37	Post-mortem iris PAD method proposed with 99% detection accuracy	No	Yes (PAD solution)
Trokielewicz *et al.* [49]	2019	37	Study of iris feature perception from human and machine perspective; trained CNN and humans use different regions in post-mortem iris classification.	No	Yes (weights of the CNN classifier)
Trokielewicz *et al.* [39]	2019	1	Analysis and comparison of iris decomposition processes and their dynamics in NIR and visible light with guidelines for forensic practitioners.	No	No
Trokielewicz *et al.* [43]	2020	79	Post-mortem iris recognition pipeline with Gabor-based filtering and CNN-based post-mortem-specific iris segmentation.	Yes (42 subjects)	Yes (CNN model weights and source codes)
Trokielewicz *et al.* [45]	2020	79	Post-mortem-specific iris image encoding method proposed with a mixture of Gabor and CNN-generated kernels.	No	Yes (segmentation model and filtering kernels)

machine classifier prefer a 'sparse' attention or 'keypoint-based' approach, which is in contrast to a dense coding typically used, such as in Daugman's algorithm [46]. This may suggest that such sparse representations can be used in combination with more traditional approaches.

C. SUMMARY OF THE RELATED LITERATURE

Table 1 summarizes the scientific literature reviewed in this section. Every study that reports FNMR for post-mortem matching finds that it greatly exceeds the FNMR expected for live irides, namely less than 2% according to the IREX IX report [47]. Post-mortem matching evaluations suffer from very limited data available to researchers. Until 2016, there were no publicly available databases comprising iris images collected from deceased subjects. Making iris biometrics more robust against post-mortem changes only started in 2018 with proposals for convolutional neural network-based image segmentation [40], [43] and later iris-specific feature representation [44], [48].

VI. DATABASES OF PERI-MORTEM AND POST-MORTEM IRIS SAMPLES

Results presented in this paper are based on peri-mortem and post-mortem iris images collected in the near-infrared (NIR) and visible-light spectra from 213 subjects independently at two institutions: Dutchess County Medical Examiner's Office in the US (data from 134 deceased subjects, referred further as *DCMEO1* dataset), and Medical University of Warsaw in Poland (referred further as *Warsaw* dataset). To our knowledge, this is the largest number of cases used in assessment of automatic post-mortem iris recognition in research publications.

A. DATA COLLECTION SITES AND PROTOCOLS

1) DUTCHESS COUNTY MEDICAL EXAMINER's OFFICE

a: EQUIPMENT

Two different sensors were used to collect DCMEO1 data: a commercial IriShield M2120U iris sensor, and the Microsoft Surface Go 8 megapixel rear-facing autofocus camera. The IriShield sensor is equipped with a NIR illuminant, whose irradiance falls in the 710-870 nm band, with a peak at 810 nm and 3dB bandwidth of 20nm (from 800 nm to 820 nm) [50].

b: ENVIRONMENTAL CONDITIONS

The bodies at the Dutchess County Medical Examiner's Office are stored at 47.8° Fahrenheit (8.8° Celsius), and were taken out of storage for a short time to take pictures in a room temperature at 72° Fahrenheit (22° Celsius).

c: WITHIN-SESSION ACQUISITION PROTOCOL

The Dutchess County operating procedure was to do one image acquisition session initially before the vitreous fluid is withdrawn and replaced with 10% buffered formalin. Thus, the subsequent sessions would already have formalin in the globes. The first RGB images are captured via camera prior to scanning the irides in NIR light. An eyelid speculum is used to facilitate the acquisition of the images. An eyedrop solution (VISINE® Advanced Relief Eyedrops) is applied

onto the surface of the cornea prior to image capture in order to moisten the cornea and improve clarity. A set of four images per eye is taken for each session. Images are labeled by a session number, a designation for the right or left eye, the postmortem time interval and whether formalin had been injected into the globe prior prior to image acquisition.

This is followed by scanning sessions using the IriTech iris sensor. An eyelid speculum is again used to facilitate the acquisition of the images and eyedrop solution applied. The iris of each globe is then scanned and the resulting ISO-complaint iris image is stored, along with the auxiliary data as for color images.

d: ACQUISITION TIMEFRAME

Once the iris is enrolled, a set of four additional images are scanned for the first session and every subsequent session on successive days. Depending on the subject, from 1 to 9 acquisition sessions could be organized on different days. The longest PMI was 284 hours in the DCMEO1 dataset.

2) MEDICAL UNIVERSITY OF WARSAW

At the Warsaw collection site, the iris scans were obtained from hospital mortuary subjects. The collection of this database was carried out in close collaboration with the Department of Ophthalmology at the Medical University of Warsaw, it had an institutional review board clearance and the ethical principles of the Helsinki Declaration were carefully followed by the researchers.

We aimed at acquiring iris images as soon after death as possible, and then repeated the acquisition multiple times (until approximately 1 month after demise) from the same subjects. First acquisition was always made right after bringing the cadaver to the mortuary, hence the bodies had often artifacts visualizing the last moments of their life: e.g., electrodes and tubes left after unsuccessful resuscitation, or other artifacts.

a: EQUIPMENT

As in case of the *DCMEO1* dataset, two different sensors were used: a commercial IriShield M2120U iris scanner, and the Olympus TG-3 color camera. Color images were collected simultaneously with NIR images, and each subject and each acquisition session is represented by at least one image of each type.

b: ENVIRONMENTAL CONDITIONS

All acquisition sessions were conducted in the hospital mortuary. The temperature in the mortuary room was approximately 42.8° Fahrenheit (6° Celsius). Other conditions, such as air pressure and humidity were unknown, yet stable. The environmental conditions in which the cadavers were kept prior to entering the cold storage are unknown.

c: WITHIN-SESSION ACQUISITION PROTOCOL

When collecting images within a single acquisition session, all samples can be considered separate presentations as recommended by the ISO/IEC 19795-2, *i.e.*, after taking a photograph, the camera was moved away from the subject and then positioned for the next acquisition.

d: ACQUISITION TIMEFRAME

Depending on the subject, 1 to 13 acquisition sessions could be organized. In each session at least one NIR and one visible-light image were acquired. Subjects were not available prior to passing, therefore no ante-mortem samples could be collected. The first session for each subject was thus always organized as soon after death as possible, typically 5 to 7 hours. The largest post-mortem interval (PMI) in Warsaw dataset is 814 hours. The following sessions were organized based on the availability of deceased persons, who were subject to medical or police investigations, and were retained in the mortuary during varying time slots. The overview of acquisition sessions for all subjects is shown in Figure 3. For 12 subjects, only a single acquisition session was possible.

B. DATA CURATION

For the Warsaw dataset, the curation involved removing failed NIR acquisitions from the dataset, such as those that did not represent the iris region, and images with significant motion blur or poor focus. The same was done for the VIS images, which were additionally cropped to only show the eye region. No curation was performed on the scans taken at the Dutchess County Medical Examiner's Office.

C. STATISTICS

The following Section summarizes the data collection protocols at both institutions and details the resulting databases of post-mortem iris representations.

1) MEDICAL UNIVERSITY OF WARSAW

The *Warsaw* dataset comprises a total of 2,294 NIR images, accompanied by 2,572 color images acquired from 79 deceased subjects (157 different irises, since only one eye was imaged for one cadaver). Age of the deceased ranged from 19 to 77 years old. 11 subjects were female and 68 were male. Causes of death included heart failure (42 subjects), car or train crash (12), suicide by hanging (11), suicide by jumping (2), unspecified type of murder (2), shooting (1), poisoning (4), and head trauma (5). The eye colors were blue/gray/light green (61 cadavers), light brown/hazel (11) and dark brown (7). This database is publicly available in version 1, an expanded version 2, and a further expanded version 3 [7], [8], [42].

2) DUTCHESS COUNTY MEDICAL EXAMINER's OFFICE

The *DCMEO1* dataset comprises a total of 621 NIR images acquired from 134 deceased subjects.

VII. IRIS RECOGNITION

This section provides a brief overview of iris recognition, as a technical context for this survey. For a more comprehensive

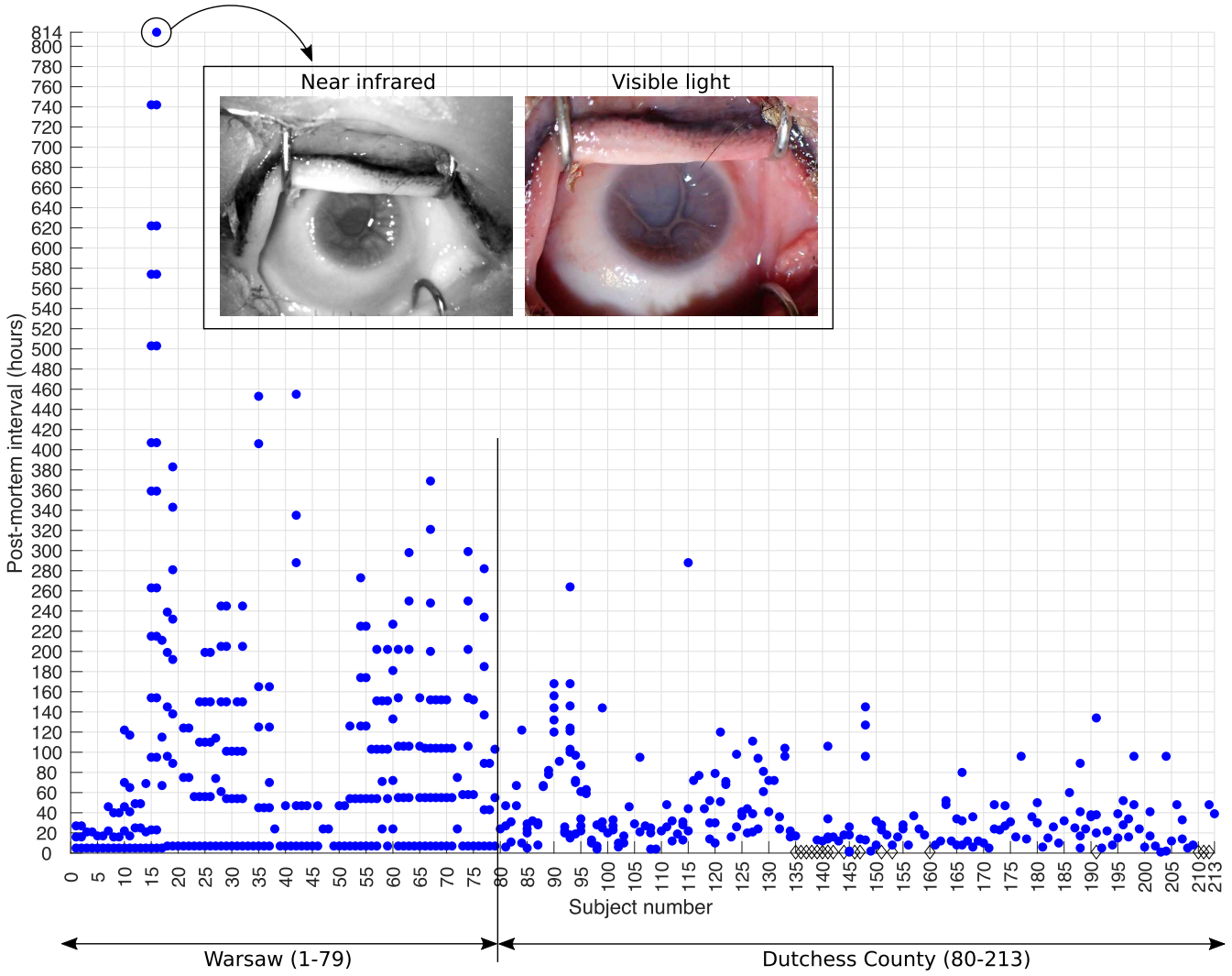

FIGURE 3. Post-mortem intervals (PMI) for all acquisition sessions plotted independently for each deceased subject from the *Warsaw* and *DCMEO1* datasets used in this study. Blue solid dots correspond to a data collection session (possibly with multiple acquisitions) for a given subject and a given PMI. Diamond shapes for some subjects denote an unknown PMI for these cases. Example NIR and visible-light samples for the subject who stayed the longest time (814 hours) in the mortuary are also shown. A clearly better penetration of the NIR light (when compared to visible light) makes the iris texture more visible in NIR. More irregular PMIs in case of *DCMEO1* data is a consequence of operational nature of acquisitions, while more regular PMIs in case of *Warsaw* data is due to more opportunities to plan an acquisition time.

treatment of iris recognition, the reader is referred to one of the recent surveys, *e.g.*, by Nguyen *et al.* [12].

The iris has a rich textural pattern that can be used as a biometric cue when appropriately captured by a sensor. Iris images are typically acquired in the near-infrared (NIR) spectrum due to the ability of NIR illumination to reliably capture the texture in dark-colored as well as light-colored irides. In 1993, Daugman published his seminal work on iris recognition which measures the statistical independence of ''iris codes'' calculated from iris images [46]. Many current commercial and academic algorithms have been inspired by early Daugman's work. The iris recognition algorithm usually comprises of four major steps:

1) *Iris Segmentation*: The first step towards iris recognition is localizing an iris from a given image. Daugman achieved this using an integrodifferential operator (circular edge detectors) to locate the outer and inner boundary of the iris [46]. Occlusion by eyelashes, eyelids, *etc.* are minimized using edge detection and curve fitting methods to estimate positions of the upper and lower eyelids.
2) *Normalization*: After localization, segmented irides are ''unwrapped'' to a fixed resolution. Unwrapping converts circular irides from Cartesian coordinate system (x, y) to polar coordinate system (r, θ). The normalization procedure reduces variations caused by pupil size and simplifies the translation needed to align two irides.
3) *Feature Encoding*: A variety of feature extraction routines exist for capturing useful textural information from an unwrapped iris. The most common techniques use various image filtering kernels, such as Gabor

filters [46], 'sticks' operators [51], or Binarized Statistical Image Features (BSIF) [48], [52], and the filtering result is then binarized to produce an ''iris code.''

4) *Matching*: In Daugman's original pipeline for iris-based recognition systems, the matching relies on the ''failure of a test of statistical independence.'' A statistical test of independence of two iris codes fails if the two iris codes belong to the same subject [46]. This is implemented using simple Boolean XOR operator that encodes disagreement between bits of given two iris codes. This information is then utilized by fractional Hamming Distance (HD) to calculate a dissimilarity score between iris samples being compared.

With recent advancements, multiple algorithms have been suggested at each of the above stages to improve the performance of iris recognition algorithms. Some of them are based on deep learning techniques, while others are combinations of both classical and deep learning-based approaches. Based on this, methods for iris recognition can be currently classified into four categories:

- *Classical*: Iris recognition algorithms in this category are mostly based on Daugman's original pipeline and some improvements that has been suggested over the years, usually proposing other than Gabor filtering kernels.. For instance, in [48] domain-specific (iris-driven) BSIF features were used instead of generic Gabor wavelets to extract textural information from iris images.
- *Fully Deep Learning-Based*: Research work has been done in this field used deep learning-based approaches [53]. Here, researchers have used convolutional neural networks to offer end-to-end iris recognition without explicit image normalization. Cosine or Euclidean distance metrics can be then used to obtain the comparison scores.
- *Hybrid with Deep Learning-Based Segmentation*: In [54], [55], authors showed that deep learning-based methods are better for iris segmentation than traditional methods, even for cases with blurred or partial iris images. This promoted the third type of algorithms for iris recognition, hybrid approaches, where iris localization and segmentation are accomplished by deep learning-based approaches, and classical approaches such as Gabor and BSIF are used for feature extraction in order to generate templates that can be matched for recognition.
- *Hybrid with Deep Learning-Based Features*: The fourth group of methods include those which employ classical iris image segmentation (and often image normalization, as in early Daugman's work), followed by deep learning-based feature encoding [56]. The motivation for using such approaches is mainly simplicity, due to the ease of feeding modern, pre-trained convolutional neural networks with normalized iris images. These methods may offer lower reliability, however, when more demanding iris image segmentation is needed, as is the case with post-mortem or diseased eyes.

In this survey, we offer an evaluation of different approaches discussed above on the post-mortem iris image datasets. Details about the iris recognition methods used in this study have been listed in Appendix and in Table 4.

VIII. EXPERIMENTAL RESULTS: WHERE ARE WE NOW?

To assess the capability of current iris recognition methodology in a context involving post-mortem samples, we evaluated it in two settings: *post-mortem vs post-mortem* (Post-Post) and *peri-mortem vs post-mortem* (Peri-Post). In the first setting, all-versus-all matching is performed only using post-mortem samples, whereas in the second setting matching is performed using *peri-mortem* images as the enrollment samples, and comparing them against all the post-mortem images from the same subjects (to generate genuine comparison scores) and against all post-mortem samples of non-mated subjects (to generate impostor comparison scores).

In trying to be as comprehensive as possible, a total of 14 different iris recognition techniques were used for matching. In some cases, variations of the same technique were also employed. Appendix contains a complete listing of the methods, along with a brief description of their workings. These methodologies can be grouped into four distinct groups as mentioned in Sec. VII and summarized in Table 4. These groups include the use of deep learning based solutions, hand-crafted techniques and commercial implementations.

The effect of iris decomposition on matching performance is studied and explained in this section. Figure 4 shows the matching scores using the best-performing method as a function of time after death for one individual subject where the segmentation of iris regions is good. Here, the reference image is matched to four other images independently. The effect of iris decomposition is apparent. Also investigated in this section is the effect of image segmentation on matching results through the examination of the failure cases of the utilized segmentation tools.

A. POST-MORTEM VS POST-MORTEM IRIS MATCHING

The Receiver Operating Characteristic (ROC) curves for the most accurate matching technique in each of the four categories of methods (as listed in Table 4) are displayed in Figure 5. The genuine/impostor lists used to generate these ROC curves contain all possible genuine and impostor comparisons where both images are post-mortem samples from the combined database of *DCMEO1* and *Warsaw* samples (these two datasets certainly contain samples from different subjects, so the merging of these two sets into a combined dataset is straightforward). This totals to $24,653$ genuine comparisons and $4,222,502$ impostor comparisons.

As seen in Figure 5, the best-performing matcher is the combination of a deep learning-based segmentation [40], feature extraction using a traditional hand-crafted method [48]

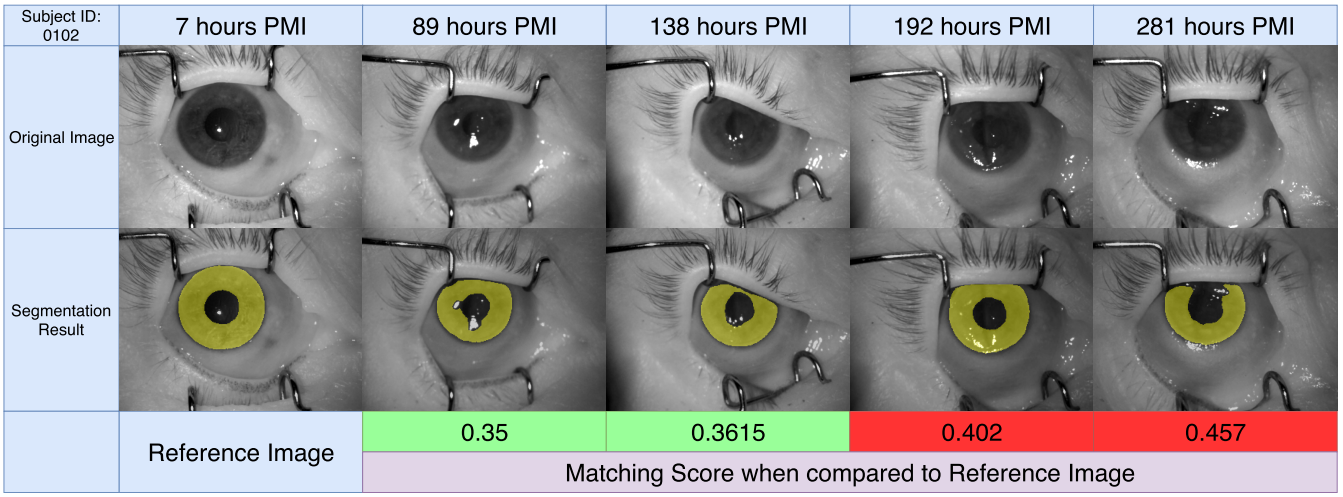

FIGURE 4. Post-mortem interval progression for one individual subject where the matching score to the reference image is shown. For the matching scores, the best-performing iris recognition method was used, (`SegNet-BSIF-HD`) and since the distance metric was Hamming Distance, lower numbers mean a better match. The acceptance threshold set on live iris images from the *CASIA-Iris-Thousand* database for a False Match Rate of 5% is used to determine whether there is a match or not. A green matching score represents a match and red represents a non-match. The matching score trend shows that as time elapses after death, matching becomes increasingly difficult.

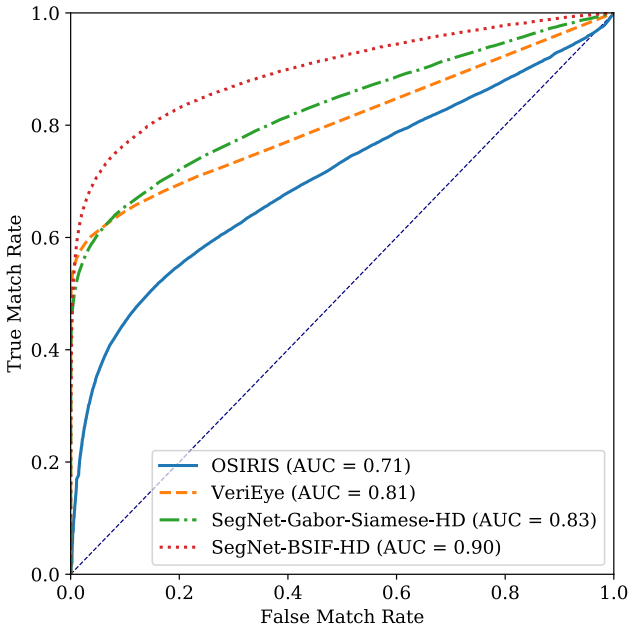

FIGURE 5. Receiver Operating Characteristic (ROC) curves for the best-performing methods in each of the four groups of iris recognition methods in the post-mortem vs post-mortem setting. Area under the curve (AUC) is also shown.

and the matching using the fractional Hamming distance as in conventional iris recognition systems. The second best-performing matcher employs the same segmentation technique, and employs a mixture of data-driven and Gabor kernels to generate an iris code. The VeriEye commercial iris recognition system was the third best-performing method. The open-source reference implementation OSIRIS offered the lowest accuracy in this experiment. However, the deep learning based-segmentation model used in the two best performing methods was trained partially on post-mortem data, which was not the case for OSIRIS or VeriEye methods. It is, therefore, evident that due to the unpredictable nature of the appearance of post-mortem irides in comparison to live irides, segmentation methods developed for live iris images tend to struggle in this domain. Since accurate segmentation plays a large role in the performance of the system, an investigation of the segmentation performance of various algorithms is presented in detail in Section VIII-F.

An interesting finding to note regarding the results shown in Figure 5 is the performance of VeriEye, the only commercial system evaluated. As can be seen in Table 2, VeriEye performs considerably better than the other techniques on live irides in the *CASIA-Iris-Thousand database* [57]. This system was clearly and understandably designed to perform recognition on live irides, and these results highlight the challenging nature of the domain of post-mortem iris recognition for such matchers.

Included in Appendix is the full set of ROC curves for all the iris matching techniques evaluated in this survey. Although this plot is dense, it can be seen that many of the methods investigated have very poor performance on the post-mortem iris recognition task. In Figure 7 it is possible to observe how the difference between genuine and impostor pairs diminishes as the PMI increases for all the techniques, reflecting degradation in the iris. A similar trend appearing in all matching techniques supports the conclusion that decay is a main factor hindering recognition in high PMI images. Specifically, we believe this to be the reason for multiple methods to perform so poorly in these conditions.

B. PERI-MORTEM VS POST-MORTEM IRIS MATCHING

The matching configuration for this experiment is that each pair contains one peri-mortem sample and the second sample

TABLE 2. Comparison of verification performance for Post-Post and Peri-Post scenarios. The acceptance thresholds (AT) were obtained at predefined False Match Rates (1% and 5%) using the *CASIA-Iris-Thousand* live iris dataset.

Methods	AT set on CASIA at FMR=1%					AT set on CASIA at FMR=5%				
	CASIA	Post-Post		Peri-Post		CASIA	Post-Post		Peri-Post	
	TMR	FMR	TMR	FMR	TMR	TMR	FMR	TMR	FMR	TMR
OSIRIS	82.41%	2.83%	27.75%	1.25%	50.00%	87.86%	4.79%	35.30%	2.08%	50.00%
USIT	19.93%	1.75%	12.42%	0.45%	0.25%	35.63%	5.79%	20.54%	3.93%	62.50%
VeriEye	99.84%	2.38%	58.54%	1.61%	87.50%	99.91%	8.29%	63.54%	6.28%	87.50%
OSIRIS-ResNet50ft-Cosine	71.37%	0.01%	17.16%	0.03%	50.00%	79.99%	0.14%	22.26%	0.28%	62.50%
OSIRIS-ResNet50ft-Euclidean	72.46%	1.00%	27.62%	0.23%	62.50%	80.82%	6.74%	34.58%	3.74%	75.00%
Segnet-Gabor-HD	79.25%	0.01%	32.28%	0.00%	50.00%	87.99%	0.19%	40.80%	0.01%	75.00%
Segnet-Gabor-Siamese-HD	83.15%	0.00%	34.76%	0.00%	50.00%	89.10%	0.06%	41.63%	0.04%	62.50%
Segnet-BSIF-HD	79.92%	0.06%	31.06%	0.01%	62.50%	85.10%	0.16%	40.96%	0.03%	62.50%
Segnet-HumanDrivenBSIF-HD	80.76%	0.80%	52.14%	0.09%	75.00%	85.65%	2.48%	62.48%	0.78%	87.50%

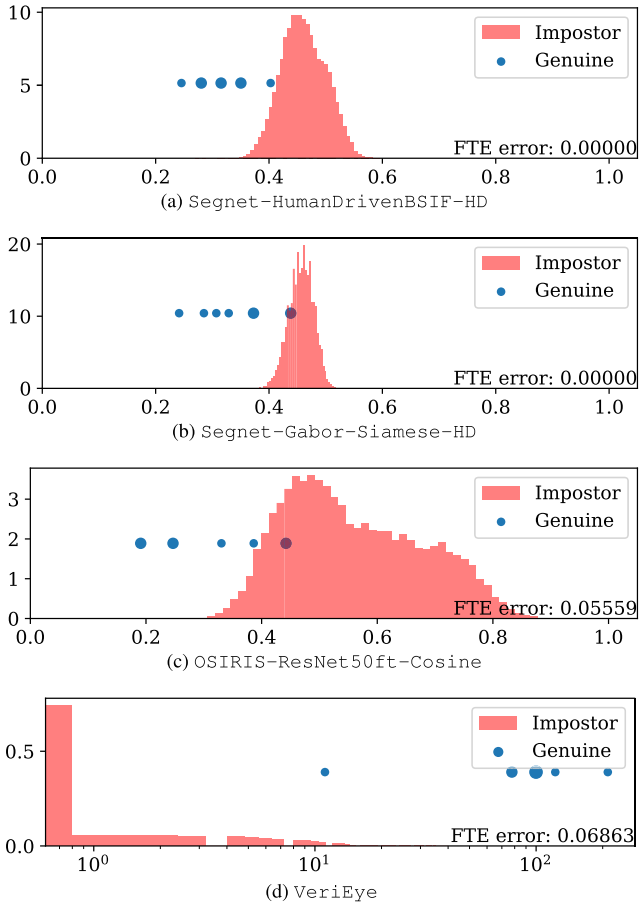

FIGURE 6. Impostor score distributions, and genuine scores shown as solid dots, for the four best-performing iris recognition methodologies in the peri-mortem vs post-mortem matching setting. Larger dots represent a higher density of genuine scores in that region.

is post-mortem. There are eight peri-mortem images in our database, thus the resulting matching lists contained only 8 genuine comparisons. The number of impostor comparisons is certainly larger, as these peri-mortem images can be compared to post-mortem samples of different subjects, and we generated 23, 360 of such scores in total. To avoid visual distortions caused by the limited number of genuine pairs available, we chose not to represent them as a histogram, but instead use dots to indicate their score relative to the larger impostor distribution, as shown in Figure 6.

In general, the matching scores attained in the peri-mortem to post-mortem setting are better than in the post-mortem to post-mortem setting. It is clear that the inclusion of live irides lends information that may be missing from post-mortem samples. In the context of post-mortem recognition, these experiments are important as they show that if a peri-mortem or standard live sample is available of a deceased subject, the matching with the post-mortem iris will produce valuable identity information. However, there is much room for improvement in this area. Firstly, as stated above, there are only 8 genuine comparisons. Increasing the size of this dataset would result in more representative results. Finally, as shown in Figure 5, currently available matching strategies do not perform well in the post-mortem to post-mortem scenario. These methods make the assumption that the whole captured iris has usable texture. However, as can be seen in Figure 10, as the iris degrades, the amount of available usable texture decreases. More minute and precise feature matching could boost the performance of both the peri-mortem to post-mortem matching and the post-mortem to post-mortem matching.

C. SETTING THRESHOLD ON LIVE IRIS IMAGES

To establish a baseline by considering the performance in a more traditional setting, we performed matching on the *CASIA-Iris-Thousand* subset of the *CASIA Iris Image Database version 4.0* [57]. The *CASIA-Iris-Thousand* database contains 2,000 classes consisting of 1,000 each of both left and right eyes. Each of these classes contains 10 images, totalling to 20,000 images. For genuine comparisons, this means there are $\binom{10}{2} = 45$ genuine comparisons per class, resulting in 90,000 total genuine comparisons. For impostor comparisons, we used a stratified sampling method, where there is at least one random comparison between each pair of impostor classes of the same side of the face, with 999 comparisons for each class (one class to all other classes of eyes on the same side of the face). This results in $2,000 \times 999 = 1{,}998{,}000$ impostor comparisons. Based on the results of this matching we then selected acceptance thresholds for two different False Match Rate values (1% and 5%), and calculated the True Match Rate (TMR) for each of them in both settings previously described (Post-Post and Peri-Post). These results are presented in Table 2.

The purpose of this experiment is to determine if we can develop a matching methodology, based on live images, that is robust to the two aforementioned settings (post-mortem vs post-mortem, and peri-mortem vs post-mortem matching). Post-mortem data is much more difficult and more expensive to collect than live data. So if it can be determined that there is a method, where a lot of post-mortem data is not required to design a robust iris recognition system, that would be preferable. When the threshold is determined on a live database and tested on that same live database, as can be seen in the CASIA column of Table 2, the commercial iris recognition system `VeriEye` performs the best by a noticeable margin. This is to be expected as this system is engineered for highly accurate iris recognition. After `VeriEye`, the next best method is the use of deep learning based segmentation and the mixture of data-driven kernels and Gabor kernels (`Segnet-Gabor-Siamese-HD`). At both an FMR of 1% and an FMR of 5%, these two matchers are the best when testing on live data. When these same thresholds are employed for post-mortem vs post-mortem comparisons, the best system is `VeriEye`, which attains a TMR of 58.54% and 63.54% at an FMR of 1% and 5%, respectively. Closely following this accuracy are the results when using the deep learning-based segmentation and human-driven BSIF features, attaining a TMR of 52.14% and 62.48% at an FMR of 1% and 5%, respectively. Beyond these two techniques, the dropoff of accuracy is very large, with the third best method only attaining a TMR of 34.76% and 41.63% at these FMRs.

In the peri-mortem vs post-mortem setting, the same matchers are the best as in the post-mortem vs post-mortem matching scenario. Since there are only eight genuine comparisons, there are many similarly performing methodologies. `VeriEye` and `Segnet-HumanDrivenBSIF-HD`, however, clearly perform better than the rest. Interestingly, when using live iris data to set matching thresholds, `VeriEye` is the best. However, when there is post-mortem data involved in the setting of thresholds, it is not the best performing method in either setting, as illustrated in the ROC curves plot in Figure 5. Given these very poor results of post-mortem iris recognition, in comparison to matching live irides, it can be concluded that using live images alone to determine matching thresholds for post-mortem recognition does not result in robust systems.

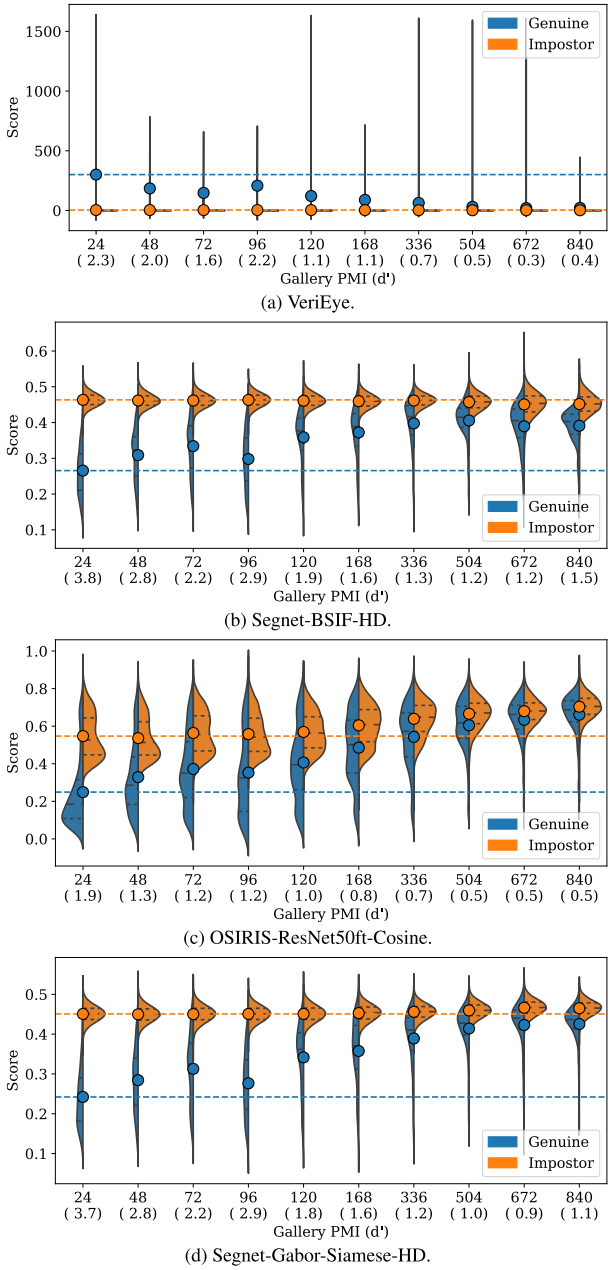

FIGURE 7. Score distributions grouped by postmortem interval (PMI). The two halves of each violin plot represent the distribution of scores for genuine and impostor pairs. Dotted lines represent the mean score for PMI up to 24 hours. d' is also shown in round brackets for each PMI range.

D. POST-MORTEM INTERVAL ANALYSIS

One of the main aspects in which post-mortem iris recognition differs from live iris recognition has to do with the significant and relatively fast image degradation due to the decomposition processes, which degrades the ocular globe and its internal structures. To assess the degree to which decomposition affects the recognition performance, we looked into the matching scores grouped by the number of hours passed since the time of death, also known as post-mortem interval (PMI). Figure 7 summarizes our findings in this regard: the violin plots show comparison score distributions obtained for samples with different PMI intervals, ranging from 24 to 840 hours. The circles represent the mean value for each PMI range, and

$$d' = \frac{|\bar{x}_{\text{genuine}} - \bar{x}_{\text{impostor}}|}{\sqrt{\frac{1}{2}(s^2_{\text{genuine}} + s^2_{\text{impostor}})}}$$

is the so-called *decidability* factor, where $\bar{x}_{\text{genuine}}$ and $\bar{x}_{\text{impostor}}$ are means, and s_{genuine} and s_{impostor} are standard deviations of the comparison scores.

The distinctive trend to be noticed here is the increasing similarity between the genuine (blue) and impostor (orange) distributions: in all methods examined, there is a clear trend in overlapping the genuine and impostor distributions, as the PMI increases, and consequently making recognition harder. In top performing methods like those shown in Figures 7b and 7d, we can observe impostor distributions concentrated around a value that remains reasonably stable across the PMI axis. On the other hand, we find genuine distributions to be well separated from the impostor when matching images with lower PMIs, but they tend to move towards and concentrate around the impostor score range as the eye starts to decay. Although this trend is not so accentuated, it is still noticeable in Figures 7a and 7c, and helps to provide a frame of reference for how the decomposition process affects iris recognition efficacy in postmortem scenarios.

E. SCORE-LEVEL FUSION IN POST-MORTEM IRIS RECOGNITION

Biometric fusion involves mixing multiple sources of information to render a single, combined decision or match score [58]. The sources of information can be multiple biometric modes, multiple matchers, feature extractors, or sensors. There are many schemes to combine the disparate information, including methods at the feature-level, at the score-level, or at the decision-level. Score-level fusion is often chosen because of its trade-off between amount of information available and ease of fusion. In score-level fusion, multiple match scores are combined to generate a new match score that may offer improved recognition performance. Singh *et al.* provide a comprehensive survey of biometric fusion [59].

Our fusion scheme combines the 14 methods described in Appendix using score-level fusion. We consider each matcher pair, resulting in $\binom{26}{2} = 365$ possible choices (some of the 14 methods have multiple distance metrics resulting in 26 matchers). To combine the scores, the score values must exist in the same range (for the sum-rule), so we use min-max normalization so that all comparison score exist in the range [0, 1]. Some matchers produce similarity scores and some matchers produce distance scores; we transform the distance scores into similarity scores by subtracting the distance scores from 1. This ensures that higher scores indicate similarity for all matchers (and thus may be easily combined by addition).

For some matchers, min-max normalization creates a problem whereby a large majority of scores exist in a very small range within [0, 1]. To help alleviate this problem, we perform z-score normalization whereby the mean comparison score is subtracted from each score and then divided by the standard deviation of the scores, *i.e.*,

$$z = \frac{x - \mu}{\sigma}$$

where, x is a comparison score, μ is the mean of the comparison scores, σ is the standard deviation of the scores, and z is the resulting normalized comparison score. The last step is the fusion of the scores from multiple matchers where corresponding scores are simply summed to produce a single combined score.

Table 3 lists the best-performing fused matchers. We follow the protocol as described in Section VIII-C, where a threshold is determined using the *CASIA-Iris-Thousand* live iris dataset.

F. SEGMENTATION ANALYSIS OF FAILURE CASES

Segmentation is an important part of the iris recognition process, and low-quality segmentation is often associated with sub-par recognition accuracy. In postmortem iris recognition, new aspects that may directly impact segmentation are introduced, mainly due to the decomposition process. To better understand how iris recognition can be applied in such scenarios, as well as the factors that impact its accuracy, we performed an analysis of segmentation results for selected failure cases. Specifically, we inspect the segmentation results for False Match (FM) and False Non-Match (FNM) errors that occurred for multiple matchers. A False Match error occurs when an impostor probe image is incorrectly matched to a gallery image, due to a low distance score (or a high similarity score, depending on the metric used by the matcher). Conversely, a False Non-Match error occurs when a genuine probe image fails to be matched with its correspondent gallery image.

The main reasons for inaccurate segmentation results in case of `OSIRIS` and `CAHT`, and possibly also `VeriEye`, are strong assumptions about geometrical and reflective properties of iris. One of the most important assumptions, significantly simplifying iris image processing, is the circularity of the iris inner and outer boundaries, which is a good approximation in case of live or peri-mortem irises. Indeed, for low PMI images, segmentation methods making this assumption work well, as shown for instance in the lower row in Figure 8bb. Similar assumptions related to shape of eyelids, or density / darkness of eyelashes, may further facilitate live iris segmentation, but impacts the accuracy of post-mortem iris image processing, as neither the shape of eyelids (deformed by metal retractors), nor properties of eyelashes covering the iris texture (due to post-mortem changes to the eyelid tissues) can be precisely predicted. The next important reason why segmentation of post-mortem iris images may be limited, when ''classical'' iris segmentation methods are used, is the decomposition processes that introduce deformations never before seen by those methods: wrinkles due to tissue drying and autolysis (*e.g.*, Figure 8ba, upper row), multiple specular reflections within the iris annulus (*e.g.*, Figure 8bc, upper row), or cornea cloudiness (*e.g.*, Figure 8ba). These examples simply call for image processing methods that have these strong assumptions relaxed, as the proposed deep learning-based method (SegNet; cf. last columns in Figures 8b and 8d).

Consequently, we inspect the results for each of these four segmentation tools trying to determine whether bad

TABLE 3. Some results of fusion using a threshold obtained on the *CASIA-Iris-Thousand* live iris dataset. The acceptance threshold (AT) is obtained at a False Match Rate (FMR) of 1% and 5% on the CASIA iris dataset.

	Fused Methods	AT set on CASIA at FMR=1%			AT set on CASIA at FMR=5%		
		CASIA TMR	FMR	TMR	CASIA TMR	FMR	TMR
Post-Post	VeriEye + Segnet-BSIF-HD	97.5%	8.19%	73.7%	98.5%	17.5%	80.5%
	VeriEye + Segnet-Gabor-Siamese-HD	99.0%	10.6%	67.4%	99.5%	22.0%	73.6%
	Segnet-Gabor-Siamese-HD + Segnet-BSIF-HD	82.9%	2.70%	64.9%	87.6%	9.73%	74.4%
	Segnet-Gabor-HD + Segnet-BSIF-HD	83.2%	2.56%	64.9%	88.3%	9.61%	75.2%
	VeriEye + Segnet-Gabor-HD	99.0%	8.56%	65.1%	99.6%	20.2%	72.6%
Peri-Post	USIT + VeriEye	83.5%	5.24%	87.5%	90.9%	11.2%	100%
	Segnet-Gabor-HD + Segnet-BSIF-HD	83.2%	6.59%	87.5%	88.3%	16.1%	87.5%
	Segnet-Gabor-Siamese-HD + Segnet-BSIF-HD	82.9%	9.11%	87.5%	87.6%	19.1%	87.5%
	OSIRIS + VeriEye	97.2%	11.2%	87.5%	98.5%	17.7%	87.5%
	USIT + Segnet-BSIF-HD	41.6%	0.00429%	50.0%	71.8%	5.51%	100%

segmentation or eye decomposition may have caused the incorrect result. Figure 8 shows some of these cases. In Figure 8a, it is clear how the advanced decay of the eyeball obscures most of the iris features, and makes segmentation harder by deforming the eye structure. On the other hand, even when the eye deformation is not so severe to the point of disturbing segmentation, clouding of the cornea may be enough to cause recognition to fail in a genuine pair (Figure 8b).

The pair shown in Figure 8c is interesting because it had different outcomes for different methodologies: both images present visible deterioration of the eye. OSIRIS and SegNet segmentation segmented the top image reasonably well, but had problems with the bottom image. CAHT located the iris incorrectly in both images, while VeriEye failed to segment them (important to notice, has different implications in performance). While OSIRIS and CAHT had segmentation problems, they did not cause a matching error for any of the matchers that used those results: they correctly classified the pair as a Non-Match. On the other hand, several matchers that used SegNet generated a False Match output. This can be explained by the particularly small region obtained from the bottom image – not enough to allow a thorough comparison between both irides. Similarly, Figure 8d had varying segmentation results, especially for the bottom image, which is severely degraded. Again, SegNet-based matchers produced a False Match due to the insufficient region segmented in the bottom image.

Visual inspection of failure cases was helpful to confirm the effect of post-mortem interval on iris segmentation and recognition. At the same time, it gives us insight on how to deal with these failures and, consequently, improve recognition quality. Unlike VeriEye, which refuses to generate bad segmentation outputs, the SegNet method always generates a binary mask as the output of this process. False Match errors are a type of error that can be particularly harmful in some applications, and cases like the ones shown in Figures 8c and 8d suggest the need to assess segmentation quality and/or the amount of iris texture left for feature extraction before matching, to mitigate these problems.

Another important factor, somewhat neglected in presented research efforts to date, is related to post-mortem iris image acquisition. Note that imaging technique designed for *live* irides was used in this study. The question is what properties of the acquisition process can be tuned to make the segmentation and iris texture coding processes more accurate? One factor is illumination wavelength and possible fusion of multi-spectral captures. While diffused illumination will not help in avoiding specularities from still-moist yet deformed cornea, applying polarized light could potentially attenuate such reflections. Although medical reasons of decomposition-driven changes to the eye are known, they have not yet been studied from a biometrics perspective. Analysis of factors such us gender, age or even reason of death brought inconclusive results regarding their potential influence on iris decomposition processes, which in turn have an impact on iris recognition [8].

Similarly, images that caused the highest number of FM and FNM errors in matching using the fusion of scores also seem to have suffered from incorrect segmentations, as can be seen in Figures 9a and 9b. In both cases, we can see that the gallery image (top row) is heavily degraded, and this causes segmentation to either a) fail completely, b) localize a wrong area (evident in ORISIS and CAHT segmentation), or c) localize an area that is too small (Figure 9a, SegNet, top row) or insufficient for a reliable comparison (Figure 9b, SegNet, top row).

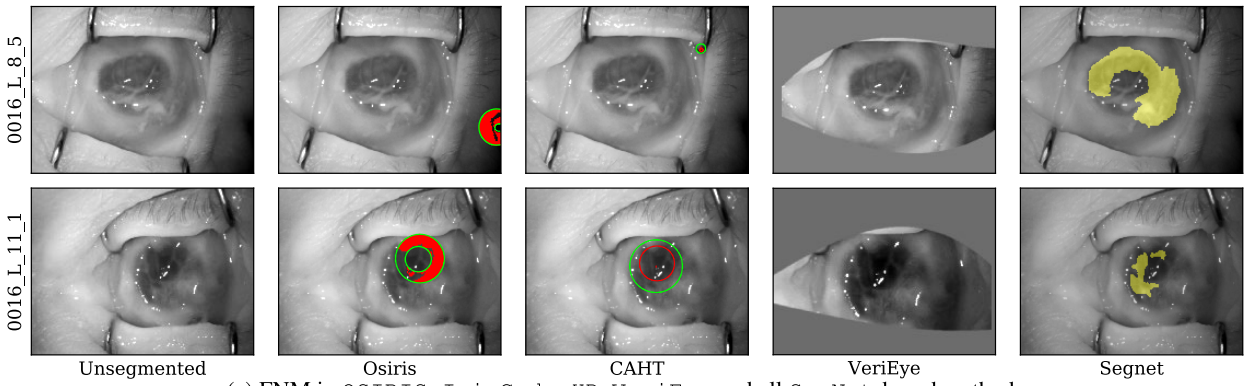

(a) FNM in `OSIRIS-IrisCode-HD`, `VeriEye` and all `SegNet`-based methods.

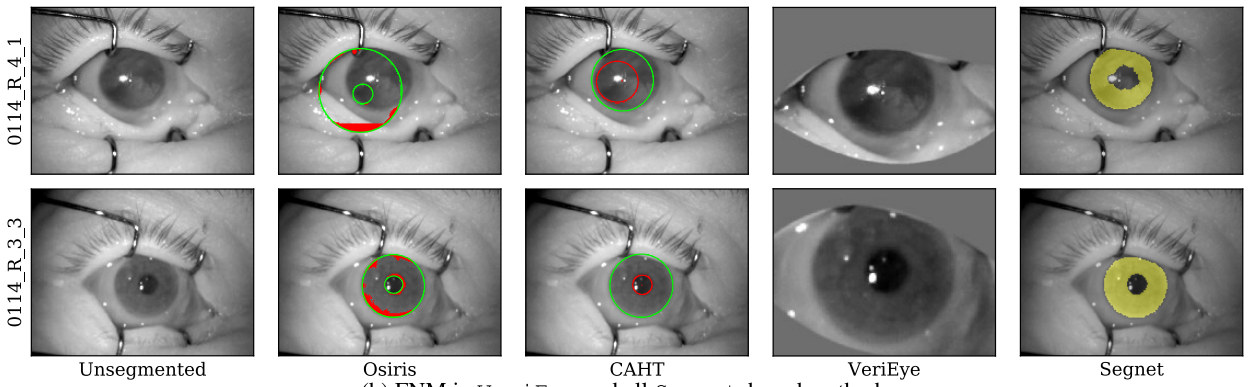

(b) FNM in `VeriEye` and all `Segnet`-based methods.

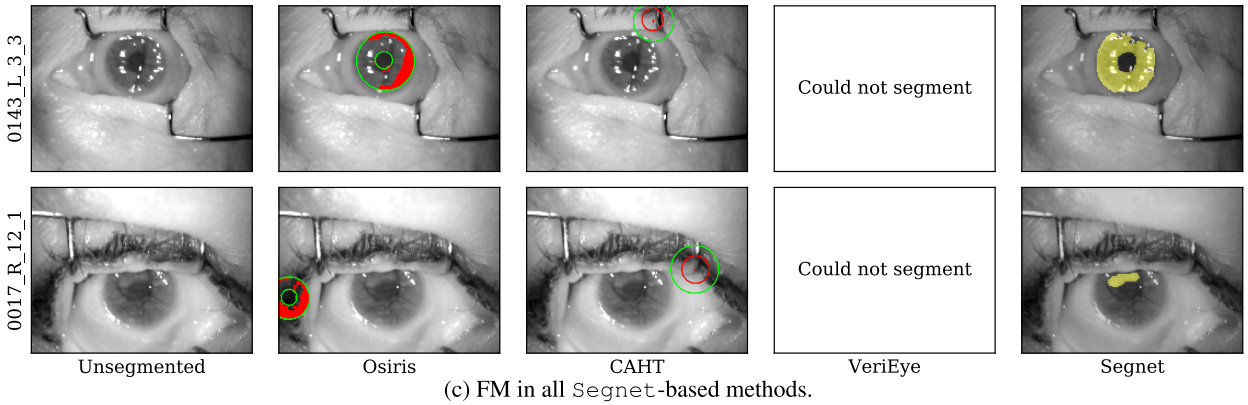

(c) FM in all `Segnet`-based methods.

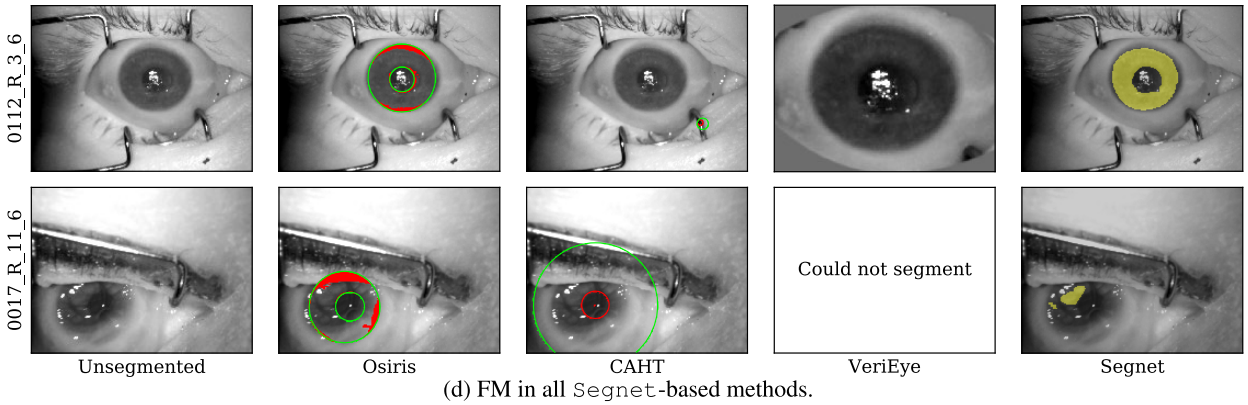

(d) FM in all `Segnet`-based methods.

FIGURE 8. **Visual analysis of failure cases: pairs that resulted in False Match (FM) or False Non-Match (FNM) errors in multiple matching methods frequently had incorrect segmentation results.**

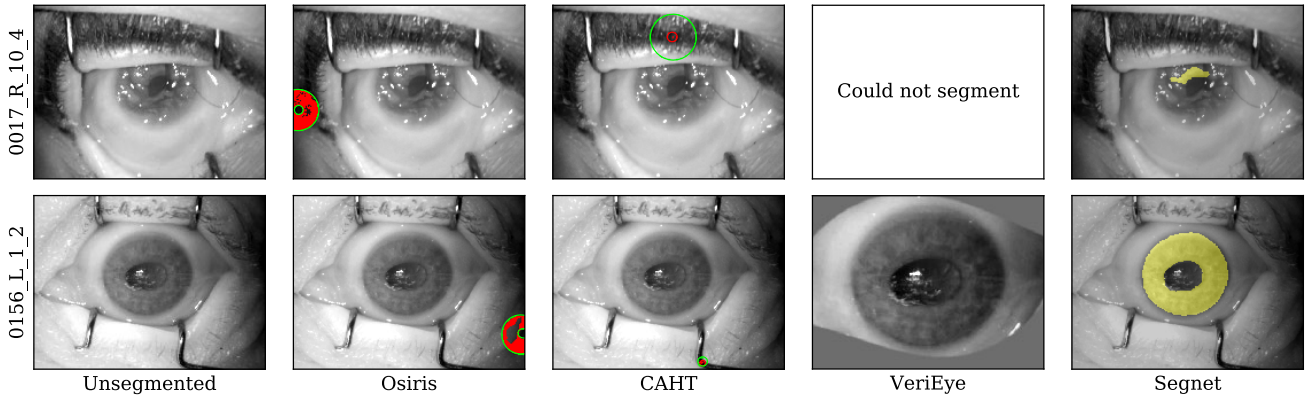

(a) FM in fusion-based method.

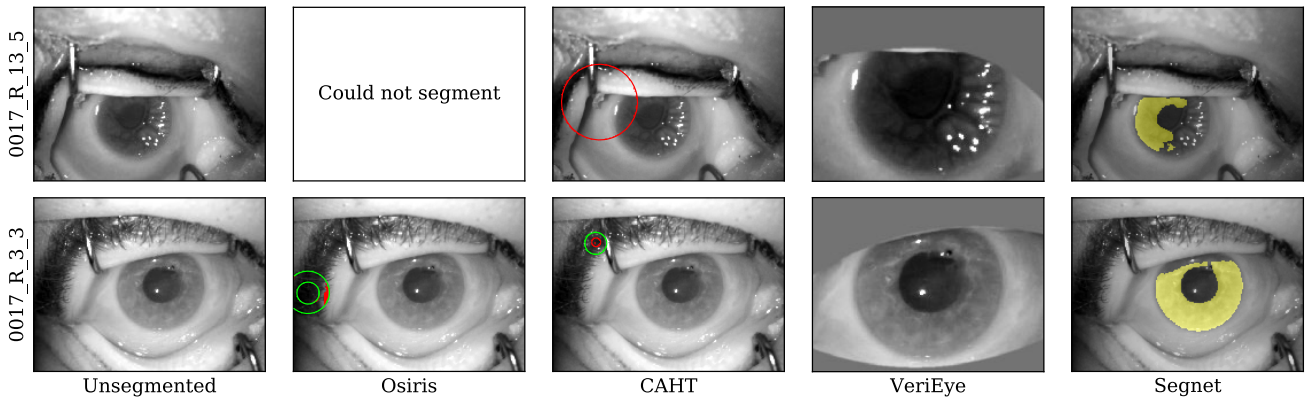

(b) FNM in fusion-based method.

FIGURE 9. Same as in Figure 8, except that matching by fusion of scores is considered..

IX. LIMITATIONS OF THE STUDY

The main limitation of this study is related to the size of the database. The current dataset consists of data from 213 subjects. We concede this limitation, and conducted our experiments and analysis with this limitation in mind. The obvious problem is the extreme difficulty of data acquisition in, what we consider to be, a very unusual setup. As these are post-mortem samples, access to the subjects is restricted to trained professionals. However, to our knowledge, this survey employs all post-mortem iris images available to researchers at the time of writing this paper. However, data collection efforts are ongoing, and, depending on the number of available cadaver subjects (which are very unpredictable), future work will extend the genuine and impostor comparison lists in both the peri-mortem versue post-mortem and post-mortem versus post-mortem settings to verify the findings presented in this paper.

Another limitation of this study has to do with the mortuary conditions. Different institutions have different practices on where the cadavers are examined. Some institutions examine the cadavers in the temperature-regulated mortuary whereas others will bring the cadavers to an office and examine the subjects there before returning them to the mortuary. This is a variable that we cannot account for and it is not clear whether the effect of the room temperature would influence iris degradation.

This study also does not investigate whether the cause of death are a factor in the performance of iris recognition. For privacy reasons, we are not given the cause of death information for some of our samples. It is possible that events such as head trauma or asphyxiation could put more pressure on the eyes and iris than in cases where the subject died of natural causes, which may lead to irregular texture degradation. However, this was not examined in this work and is an area for future research.

Finally, the sensor used to capture the images was designed to capture live irides. This device has a mirror on the surface facing the subject in order for them to align themselves with this camera. However, in the case of our work, the individual capturing the image must do this alignment. There is an LED to notify the user when the image is aligned; however, it is possible that the irregular texture and shape of post-mortem irides may affect the operation of this process. Thus, it is possible that acquired images are not of the same quality as live iris samples which are well-aligned. Last but not the least, we do not yet know if the near-infrared illumination (with a power peak in 810 nm), which is optimal for acquisition of live irides, is still the effective choice to acquire the best

representation for cadaver irides. This has been also identified by the authors as an important future research area.

X. CONCLUSIONS

The subject of post-mortem biometric recognition has gained traction in several applications. In particular, the ability to recognize deceased individuals in mass disasters or in urban warfare has expedited the need to develop biometric recognition algorithms that can successfully match post-mortem biometric data with their ante-mortem and peri-mortem counterparts. In this paper, we focused on the efficacy of state-of-the-art iris recognition algorithms – primarily developed for ''live'' irides – on the processing and matching of PM data, and evaluated a few of the most recent algorithms adapted to PM iris recognition. This survey paper and the assessment presented are unique in several ways:

- In addition to a comprehensive literature review related to post-mortem iris recognition, this survey presents a new study with more than 20 iris recognition methods.
- Our study presented in this paper uses a large database of more than 3,000 post-mortem iris images acquired in near-infrared light from 213 deceased subjects; the acquisitions were organized by two different facilities located in the US and in Europe. It is the largest known to us database of peri-mortem and post-mortem iris images used in published research to date.
- We present matching results between iris images acquired before and after death of the same subjects.

Several important observations can be formulated after completing this study:

- State-of-the-art iris recognition methods, designed to process live iris images, are not yet prepared to address adequately post-mortem eye deformations. This is especially evident after analysing image segmentation results, which is the main reason for matching failures. Solutions with relaxed assumptions related to the iris shape (*e.g.*, models incorporating convolutional neural networks or geodesic active contours [60]) seem to offer a promising direction of adapting current method to forensic applications.
- Comparing peri-mortem with corresponding post-mortem iris images results in correct matching in some cases. This gives a hope that post-mortem samples can be used in a forensic setup in which live iris samples need to be matched to their post-mortem counterparts.
- The existing iris recognition matchers offer very different accuracy values when applied to post-mortem iris data. We have shown in this study that fusion of the best methods can serve as an immediate solution to increase the reliability of subjects' identification after demise with the use of their iris patterns.

XI. FUTURE DIRECTIONS

As concluding remarks, we itemize a number of research opportunities in the area of post-mortem iris recognition.

1) Developing specialized methods for segmenting the iris from post-mortem ocular data: As discussed in an earlier section, post-mortem changes in the iris can impact the limbus and the pupillary boundaries, besides modifying the perceived texture and shape of the iris. This necessitates the development of new iris segmentation algorithm, especially because iris segmentation is one of the most critical components in the recognition pipeline.
2) Developing methods for encoding and matching post-mortem irides: In many post-mortem scenarios, the quality of the iris texture can be substantially different from that of live images. Further, only a portion of the iris may be available due to the nature of decomposition. This requires the development of new iris encoding and matching algorithms.
3) Modeling post-mortem iris texture decomposition: As discussed earlier, the process of iris decomposition depends upon a number of factors including the pathological state of the individual prior to death, cause of death, post-mortem interval, environmental conditions, etc. Predicting the changes in iris morphology and texture can benefit post-mortem iris recognition algorithms.
4) Assembling large post-mortem iris datasets: The number of datasets available for post-mortem iris recognition research is fairly limited. Further, each of these datasets have only a limited number of subjects. Curating larger datasets will not only facilitate a more systematic study on this topic, but will also provide data needed for training post-mortem iris recognition algorithms.
5) Use of post-mortem iris data as presentation attack vectors: It is not inconceivable for an adversary to utilize post-mortem iris data to launch a presentation attack against iris recognition systems. Methods to detect such attacks are necessary to enhance the security of iris systems.

APPENDIX. ILLUSTRATION OF IRIS POST-MORTEM DECOMPOSITION PROCESS

Figures 10 and 11 present a series of post-mortem iris images acquired in near infrared and visible light from the same eye until 814 hours after demise (the longest case in the combined *DCMEO1* + *Warsaw* database). All images were acquired from the same eye and show the upside of near-infrared acquisition, as this light penetrates the cloudy cornea better than visible light.

APPENDIX. IRIS RECOGNITION METHODS USED IN THIS STUDY

This Appendix lists and shortly characterizes all iris recognition methods (with their variants) used in the experiments presented in this survey paper.

1) **Neurotechnology VeriEye SDK v4.11** [61].
Name on plots: `VeriEye`.

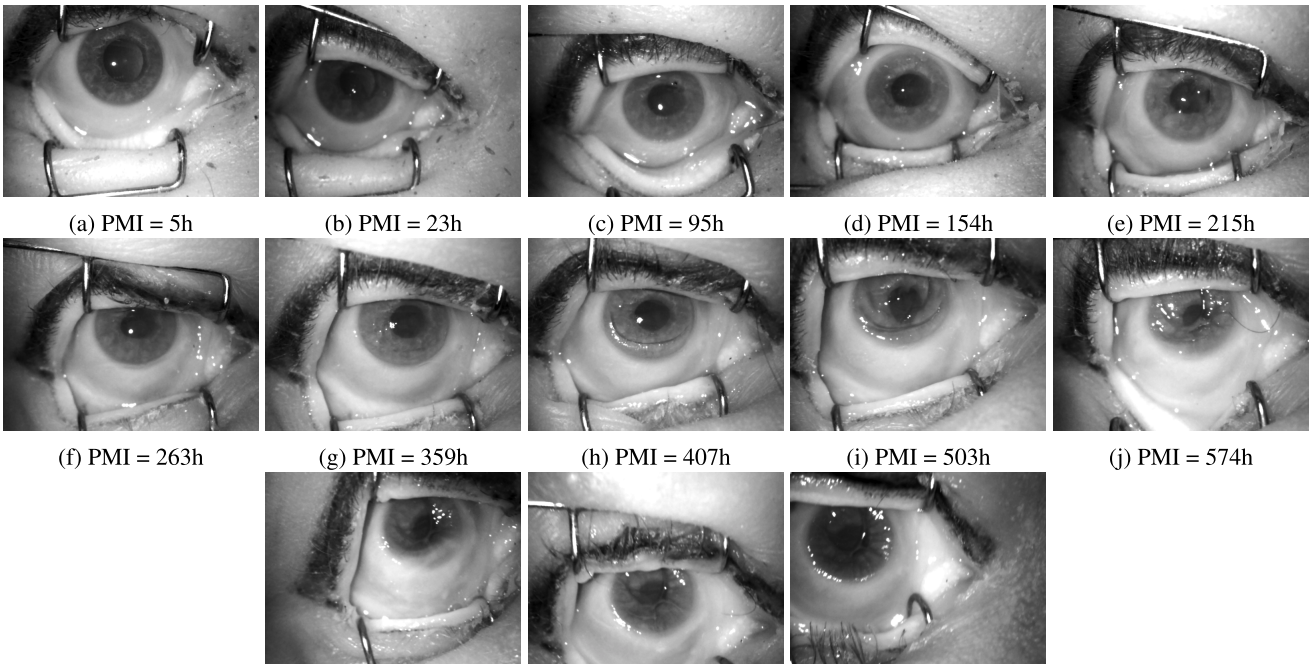

FIGURE 10. Illustration of the decomposition processes visible in near-infrared light (3dB bandwidth 790 nm – 830 nm, with a peak in 810 nm) in the right eye of subject *0017* included into the *Warsaw* data.

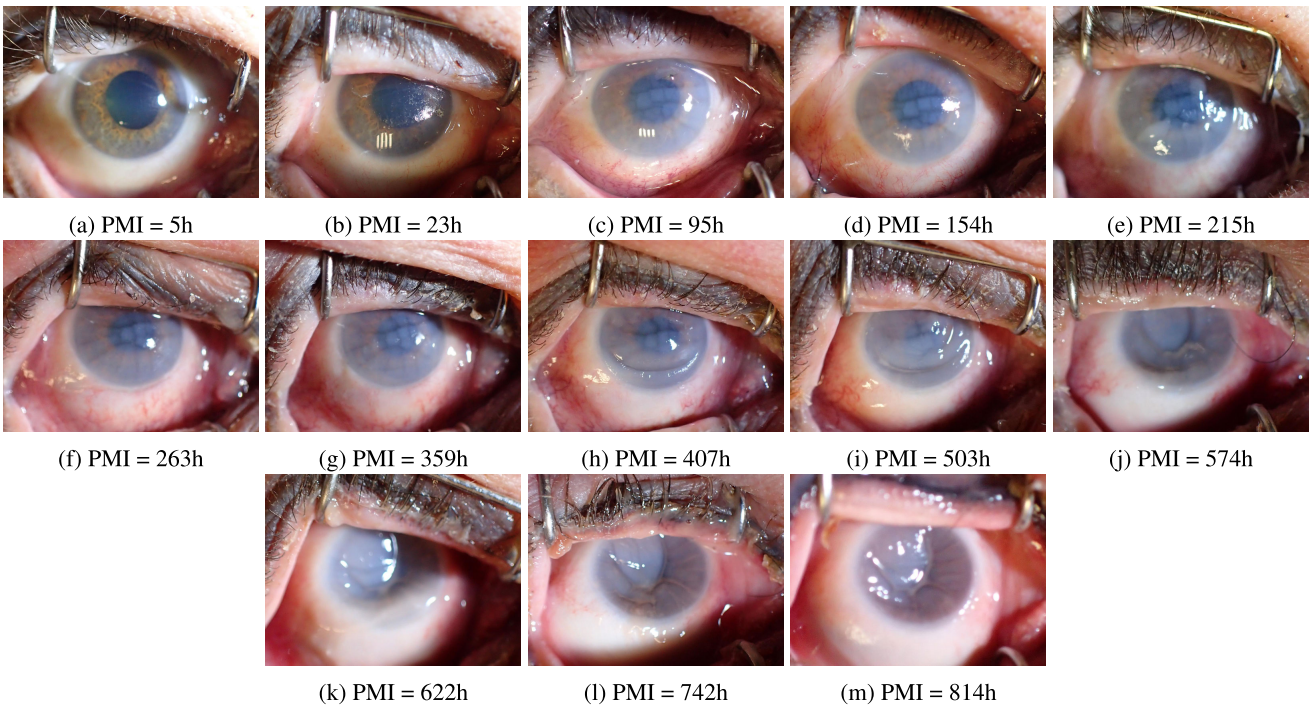

FIGURE 11. Same as in Fig. 10, except that visible-light samples are shown.

This is a commercial tool for iris recognition produced by Neurotechnology. It works by using Taylor expansion to extract image features. Features extracted from the images are compared using a metric called "elastic similarity" in which impostor images will usually produce results near zero. This SDK has been evaluated several times by NIST in their IREX reports (I, III, IV and IX), and currently is one of the most popular and

accurate commercial iris recognition methods. In particular, in 2018 the VeriEye SDK has been judged by the NIST as the second most accurate among all IREX participants.

2) **OSIRIS (Open Source IRIS) v4.1** [62].
Name on plots: `OSIRIS-IrisCode-HD`.
A very popular open-source implementation of Daugman's approach for iris recognition. It uses Gabor wavelet filtering to extract features from the iris images, and then generates the IrisCode that is used to measure the distance between two irises through fractional Hamming distance.

3) **USIT (University of Salzburg Iris Toolkit) v2** [63].
Name on plots: `CAHT-LG-TripleA`.
An open-source academic tool that implements a Daugman-style iris recognition, using iris codes to calculate the Hamming distance between images. Optimal configuration, as suggested by the authors, was used: segmentation using `CAHT`, feature extraction using `LG` and matching using `TripleA` algorithms.

VeriEye-based

4) **segmentation**
+ **OTS ResNet-18** [56]. Names on plots:
`VeriEye-ResNet18-Cosine`,
`VeriEye-ResNet18-MSE`, and
`VeriEye-ResNet18-Pairwise`.
Deep learning-based features extracted from off-the-shelf ResNet-18 for iris images segmented and normalized by `OSIRIS`.

VeriEye-based

5) **segmentation**
+ **OTS ResNet-152** [56]. Names on plots:
`VeriEye-ResNet152-Cosine`,
`VeriEye-ResNet152-MSE`, and
`VeriEye-ResNet152-Pairwise`. As above, except for ResNet-152 used for feature extraction.

OSIRIS-based

6) **segmentation**
+ **OTS DenseNet** [56]. Names on plots:
`VeriEye-DenseNet-Cosine`,
`VeriEye-DenseNet-MSE`, and
`VeriEye-DenseNet-Pairwise`.
As above, except for DenseNet used for feature extraction.

VeriEye-based

7) **segmentation**
+ **OTS VGG-16** [56]. Names on plots:
`VeriEye-VGG16-Cosine`,
`VeriEye-VGG16-MSE`, and
`VeriEye-VGG16-Pairwise`.
As above, except for VGG-16 used for feature extraction.

VeriEye-based

8) **segmentation**
+ **OTS AlexNet** [56]. Names on plots:
`VeriEye-AlexNet-Cosine`,
`VeriEye-AlexNet-MSE`, and
`VeriEye-AlexNet-Pairwise`.
As above, except for AlexNet used for feature extraction.

OSIRIS-based

9) **segmentation**
+ **fine-tuned ResNet50** [64]. Names on plots:
`OSIRIS-ResNet50ft-Cosine`, and
`OSIRIS-ResNet50ft-Euclidean`.
The approach is to fine-tune the popular ResNet-50 architecture trained originally on ImageNet database for the task of iris recognition using a large live iris database. Using this trained network, features are extracted from each of the convolutional layers and tested using a multiclass SVM to select which layer is the best feature extractor. For this project, the best performing layer and network configuration proposed in [64] was used to extract the features from the post-mortem images. All images are normalized using OSIRIS and these normalized images provided the input to the network. Because the original methodology was for the task of iris classification, and this project is dealing with iris verification, an SVM could not be used on the features. Instead, the features extracted for each image were matched using the Euclidean distance and in a second experiment the cosine distance between the feature vectors was used.

SegNet-based

10) **segmentation**
+ **Gabor kernels** [40], [45]. Name on plots:
`SegNet-Gabor-HD`.
A deep learning-based (SegNet) iris image segmentation designed in the past specifically for post-mortem iris image processing and Gabor kernels (as defined in OSIRIS). Standard iriscode-based matching (fractional Hamming distance, occlusions excluded, but without 'fragile bits' analysis).

SegNet-based

11) **segmentation**
+ **mixture of Gabor + Siamese kernels** [40], [44]. Name on plots:
`SegNet-Gabor+Siamese-HD`.
As above, except for a mixture of Gabor and data-driven (learned by Siamese networks) kernels used for feature extraction.

SegNet-based

12) **segmentation**
+ **standard BSIF** [40]. Name on plots:
`SegNet-BSIF-HD`.
As above, except for using standard Binary Statistical Image Features (BSIF) as proposed by Kannala and Rathu [65] to extract features.

SegNet-based

13) **segmentation**
+ **human-driven BSIF** [40], [48]. Name on plots:
`SegNet-HumanDrivenBSIF-HD`.

TABLE 4. Proposed categorization of the recognition methods employed.

Classic Segmentation, Classic Encoding	VeriEye OSIRIS-IrisCode-HD CAHT-LG-TripleA
CNN Segmentation, Classic Encoding	Segnet-Gabor-HD Segnet-BSIF-HD Segnet-HumanDrivenBSIF-HD Segnet-Crypts-Dissimilarity Segnet-Crypts-Number
Classic Segmentation, CNN Encoding	OSIRIS-ResNet50ft-Cosine OSIRIS-ResNet50ft-Euclidean VeriEye-ResNet18-Cosine VeriEye-ResNet18-MSE VeriEye-ResNet18-Pairwise VeriEye-ResNet152-Cosine VeriEye-ResNet152-MSE VeriEye-ResNet152-Pairwise VeriEye-DenseNet-Cosine VeriEye-DenseNet-MSE VeriEye-DenseNet-Pairwise VeriEye-VGG16-Cosine VeriEye-VGG16-MSE VeriEye-VGG16-Pairwise VeriEye-AlexNet-Cosine VeriEye-AlexNet-MSE VeriEye-AlexNet-Pairwise
CNN Segmentation, CNN Encoding	Segnet-Gabor-Siamese-HD

A deep learning-based (SegNet) iris image segmentation and human-driven BSIF, which were obtained after applying Independent Component Analysis on iris image patches extracted from eye gaze recorded for people comparing iris samples

Human-interpretable

14) **iris crypts** [66].
Names on plots:
`SegNet-Crypts-Dissimilarity` and `SegNet-Crypts-Number`.
This matcher implements detection and automatic matching of the so-called iris crypts – features that can be easily interpreted by humans. The designed matching scheme is able to handle potential topological changes in the detection of the same crypt in different images.

For better organization, we split these methods into four categories, according to the approach that is used in the segmentation and encoding phases. This categorization is shown in Table 4.

APPENDIX. DETAILED IRIS COMPARISON RESULTS

This Appendix presents the ROC curves for all iris recognition methods used in this study. The methods were put into four categories due to several reasons:

- While the test set was identical for all matchers (as described in Section VI, the training datasets differed across the methods. Methods included into Fig. 12 are off-the-shelf algorithms, which were designed on unknown data, probably not including post-mortem iris samples. Methods presented in Fig. 13 used partially post-mortem data to train the CNN-based segmentation (SegNet), but no post-mortem samples were used to train feature encoding part. Methods used to generate Fig. 14 did not use (again: to our best knowledge) any post-mortem data to train either image segmentation or feature extraction models. Finally, the results

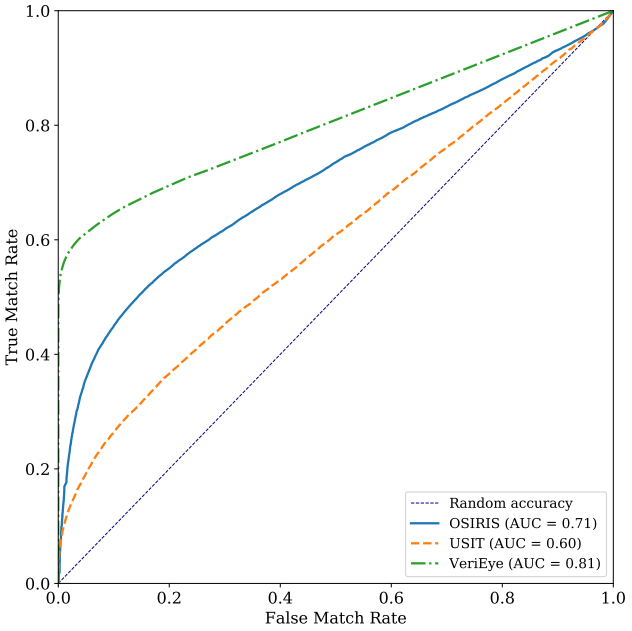

FIGURE 12. Classic segmentation, classic encoding. The three SDKs were used without any modifications. Here, the test data consisted of post-mortem iris images. `OSIRIS` **could not process 2.3% of images;** `USIT` **could not process 0.03% of images; and** `VeriEye` **could not process 6.8% of images.**

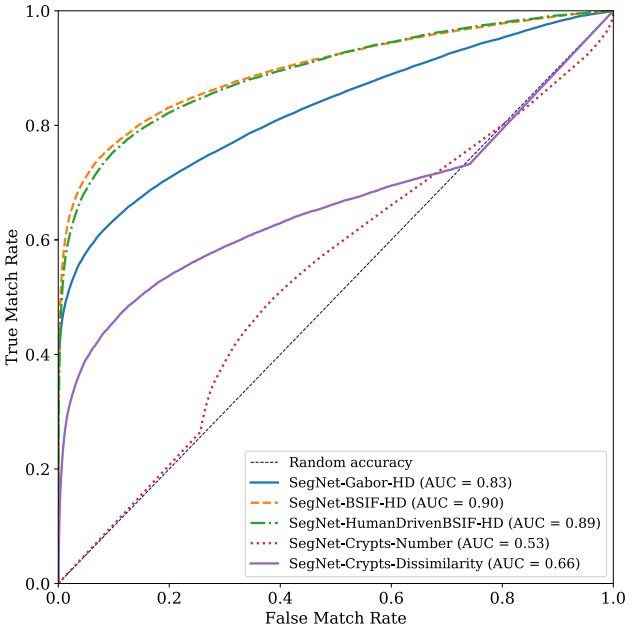

FIGURE 13. CNN segmentation and classic encoding. The training data used for the segmentation routine consisted of 2,987 post-mortem and 7,193 ante-mortem images. The test data consisted only of post-mortem images. The unusual shape of the ROC curves for the `SegNet-Crypts methods` **is due to the nature of the results: these methods present histogram spikes on either the low or the high distribution tails. When the threshold reaches that spike, the result is a straight line in the ROC curve.**

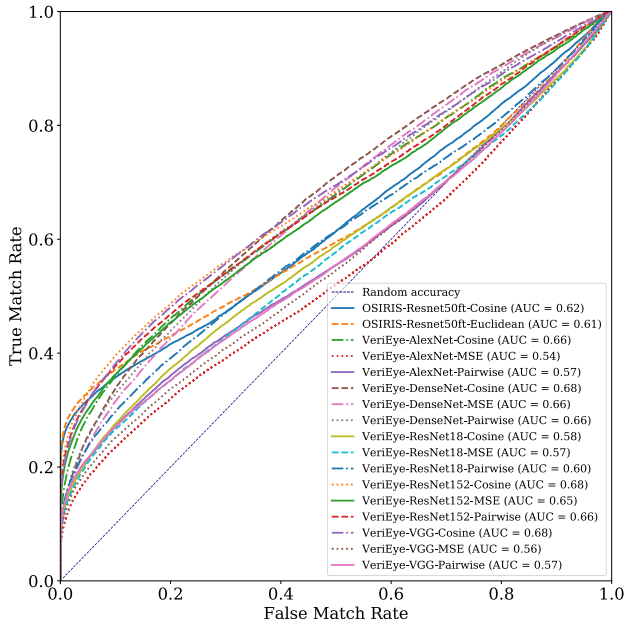

FIGURE 14. **Classic segmentation and CNN encoding. Segmentation was accomplished using two SDKs without any modifications. Encoding and matching was accomplished using various CNNs that were trained *only* on ante-mortem images. `OSIRIS` could not process 2.3% of images; and `VeriEye` could not process 5.8% of images. The poor performance of the CNNs is due to the fact that they were never trained on post-mortem images. This conveys the importance of assembling a large post-mortem dataset for training CNN-based iris encoders for post-mortem iris recognition.**

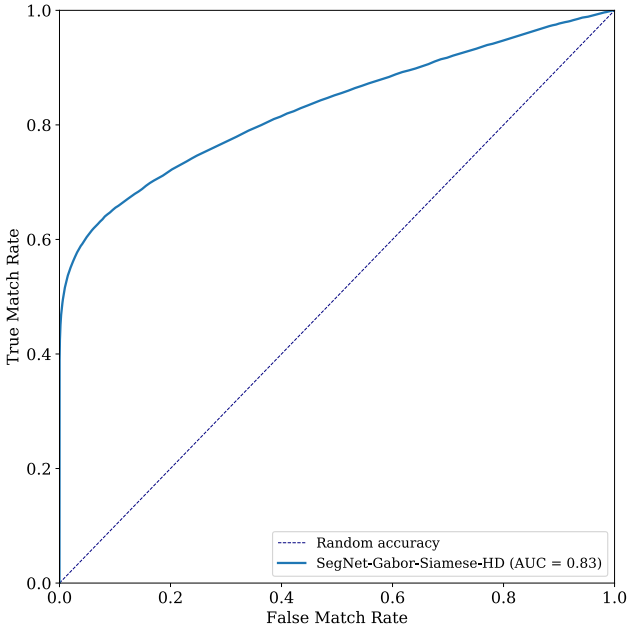

FIGURE 15. **CNN segmentation and CNN encoding. Here, segmentation was accomplished using a CNN that was trained on 2,987 post-mortem and 7,193 ante-mortem images. Encoding and matching was accomplished using another CNN that was trained on 2,475 post-mortem images. Testing was done on subject-disjoint post-mortem iris images. This ROC curve demonstrates the importance of using post-mortem images for training purposes. Contrast this with Figure 14.**

illustrated in Fig. 14 correspond to a method, which incorporated post-mortem iris images to train both image segmentation and kernels responsible for feature extraction. This is why ROCs should not be directly compared among these four Figures.

- Two core elements of the iris recognition pipeline, image segmentation and feature encoding, can employ deep learning-based models. We thus categorized all methods by the fact of using the CNN or applying classical (or "hard-crafted") models, what ends up with four groups.

It is also important to note that the SegNet (used in various methods in this study) was trained on data including post-mortem samples from the first 17 subjects in the Warsaw corpus. It means that for methods using SegNet the training and testing sets were not subject-disjoint (17 subjects, out of 213, are common between these sets). That is a consequence of how the CNN models for post-mortem iris recognition have been built in the past, with incrementally increasing size of the hard-to-collect database.

REFERENCES

[1] A. K. Jain, A. Ross, and S. Prabhakar, "An introduction to biometric recognition," *IEEE Trans. Circuits Syst. Video Technol.*, vol. 14, no. 1, pp. 4–20, Jan. 2004.

[2] A. K. Jain, K. Nandakumar, and A. Ross, "50 years of biometric research: Accomplishments, challenges, and opportunities," *Pattern Recognit. Lett.*, vol. 79, pp. 80–105, Aug. 2016.

[3] A. Ross, S. Banerjee, C. Chen, A. Chowdhury, V. Mirjalili, R. Sharma, T. Swearingen, and S. Yadav, "Some research problems in biometrics: The future beckons," in *Proc. Int. Conf. Biometrics (ICB)*. Crete, Greece: IEEE, Jun. 2019, pp. 1–6.

[4] D. S. Bolme, R. A. Tokola, C. B. Boehnen, T. B. Saul, K. A. Sauerwein, and D. W. Steadman, "Impact of environmental factors on biometric matching during human decomposition," in *Proc. IEEE 8th Int. Conf. Biometrics Theory, Appl. Syst. (BTAS)*. Niagara Falls, NY, USA: IEEE, Sep. 2016, pp. 1–8.

[5] K. Sauerwein, T. B. Saul, D. W. Steadman, and C. B. Boehnen, "The effect of decomposition on the efficacy of biometrics for positive identification," *J. Forensic Sci.*, vol. 62, no. 6, pp. 1599–1602, Nov. 2017, doi: 10.1111/1556-4029.13484.

[6] M. Trokielewicz, A. Czajka, and P. Maciejewicz, "Post-mortem human iris recognition," in *Proc. Int. Conf. Biometrics (ICB)*. Halmstad, Sweden: IEEE, Jun. 2016, pp. 1–6.

[7] M. Trokielewicz, A. Czajka, and P. Maciejewicz, "Human iris recognition in post-mortem subjects: Study and database," in *Proc. IEEE 8th Int. Conf. Biometrics Theory, Appl. Syst. (BTAS)*. Niagara Falls, NY, USA: IEEE, Sep. 2016, pp. 1–6.

[8] M. Trokielewicz, A. Czajka, and P. Maciejewicz, "Iris recognition after death," *IEEE Trans. Inf. Forensics Security*, vol. 14, no. 6, pp. 1501–1514, Jun. 2019.

[9] US Official Site, Canada Official Site. *NEXUS: Joint USA and Canada Trusted Traveler Program*. Accessed: Aug. 13, 2016. [Online]. Available: https://www.cbp.gov/travel/trusted-traveler-programs/nexus and http://www.nexus.gc.ca

[10] Unique Identification Authority of India. *AADHAAR*. Accessed: Aug. 11, 2015. [Online]. Available: http://uidai.gov.in

[11] "Ghana, Tanzania and Somaliland introduce biometric voter verification," *Biometric Technol. Today*, vol. 2015, no. 10, pp. 3–12, 2015. [Online]. Available: https://www.sciencedirect.com/science/article/pii/S096947651530151X, doi: 10.1016/S0969-4765(15)30151-X.

[12] K. Nguyen, C. Fookes, R. Jillela, S. Sridharan, and A. Ross, "Long range iris recognition: A survey," *Pattern Recognit.*, vol. 72, pp. 123–143, Dec. 2017, doi: 10.1016/j.patcog.2017.05.021.

[13] M. J. Burge and M. K. Monaco, "Multispectral iris fusion for enhancement, interoperability, and cross wavelength matching," *Proc. SPIE*, vol. 7334, pp. 494–501, Apr. 2009, doi: 10.1117/12.819058.

[14] J. Webb, D. M. Etter, V. Barboza, and E. Sharp, "Iris recognition using cross-spectral comparison," in *Proc. 50th Asilomar Conf. Signals, Syst. Comput.*, Nov. 2016, pp. 434–438.

[15] M. Trokielewicz and E. Bartuzi, "Cross-spectral iris recognition for mobile applications using high-quality color images," *J. Telecommun. Inf. Technol.*, vol. 3, pp. 91–97, Sep. 2016.

[16] S. L. Belsey and R. J. Flanagan, "Postmortem biochemistry: Current applications," *J. Forensic Legal Med.*, vol. 41, pp. 49–57, Jul. 2016, doi: 10.1016/j.jflm.2016.04.011.

[17] J. I. Coe, "Vitreous potassium as a measure of the postmortem interval: An historical review and critical evaluation," *Forensic Sci. Int.*, vol. 42, no. 3, pp. 201–213, 1989, doi: 10.1016/0379-0738(89)90087-X.

[18] S. Jaafar and L. Nokes, "Examination of the eye as a means to determine the early postmortem period: A review of the literature," *Forensic Sci. Int.*, vol. 64, no. 2, pp. 185–189, 1994, doi: 10.1016/0379-0738(94)90230-5.

[19] K. Jashnani, S. Kale, and A. Rupani, "Vitreous humor: Biochemical constituents in estimation of postmortem interval," *J. Forensic Sci.*, vol. 55, pp. 1523–1527, Nov. 2010.

[20] B. Madea, "Is there recent progress in the estimation of the postmortem interval by means of thanatochemistry?" *Forensic Sci. Int.*, vol. 151, pp. 49–139, Aug. 2005.

[21] J. W. Brooks, "Postmortem changes in animal carcasses and estimation of the postmortem interval," *Veterinary Pathol.*, vol. 53, no. 5, pp. 929–940, Sep. 2016, doi: 10.1177/0300985816629720.

[22] F. Bévalot, N. Cartiser, C. Bottinelli, L. Fanton, and J. Guitton, "Vitreous humor analysis for the detection of xenobiotics in forensic toxicology: A review," *Forensic Toxicol.*, vol. 34, no. 1, pp. 12–40, Jan. 2016.

[23] I. Cantürk and L. Özyilmaz, "A computational approach to estimate postmortem interval using opacity development of eye for human subjects," *Comput. Biol. Med.*, vol. 98, pp. 93–99, Jul. 2018.

[24] L. Fleischer, S. Sehner, A. Gehl, M. Riemer, T. Raupach, and S. Anders, "Measurement of postmortem pupil size: A new method with excellent reliability and its application to pupil changes in the early postmortem period," *J. Forensic Sci.*, vol. 62, no. 3, pp. 791–795, May 2017.

[25] M. Kaliszan, "Studies on time of death estimation in the early post mortem period—Application of a method based on eyeball temperature measurement to human bodies," *Legal Med.*, vol. 15, no. 5, pp. 278–282, Sep. 2013, doi: 10.1016/j.legalmed.2013.06.003.

[26] P. E. Napoli, M. Nioi, E. d'Aloja, and M. Fossarello, "Post-mortem corneal thickness measurements with a portable optical coherence tomography system: A reliability study," *Sci. Rep.*, vol. 6, no. 1, Sep. 2016, Art. no. 30428.

[27] G. Prieto-Bonete, M. D. Perez-Carceles, and A. Luna, "Morphological and histological changes in eye lens: Possible application for estimating postmortem interval," *Legal Med.*, vol. 17, no. 6, pp. 437–442, Nov. 2015, doi: 10.1016/j.legalmed.2015.09.002.

[28] S. Tsunenari and M. Kanda, "The roles of corneal mucopolysaccharides and water contents in post-mortem corneal clouding," *J. Forensic Sci.*, vol. 11, no. 1, pp. 87–92, 1978, doi: 10.1016/0379-0738(78)90101-9.

[29] L. Zhou, Y. Liu, L. Liu, L. Zhuo, M. Liang, F. Yang, L. Ren, and S. Zhu, "Image analysis on corneal opacity: A novel method to estimate postmortem interval in rabbits," *J. Huazhong Univ. Sci. Technol. [Med. Sci.]*, vol. 30, no. 2, pp. 235–239, Apr. 2010, doi: 10.1007/s11596-010-0221-2.

[30] K. Koehler, S. Sehner, M. Riemer, A. Gehl, T. Raupach, and S. Anders, "Post-mortem chemical excitability of the iris should not be used for forensic death time diagnosis," *Int. J. Legal Med.*, vol. 132, no. 6, pp. 1693–1697, Nov. 2018, doi: 10.1007/s00414-018-1846-0.

[31] S. Larpkrajang, W. Worasuwannarak, V. Peonim, J. Udnoon, and S. Srisont, "The use of pilocarpine eye drops for estimating the time since death," *J. Forensic Legal Med.*, vol. 39, pp. 100–103, Apr. 2016. [Online]. Available: http://www.sciencedirect.com/science/article/pii/S1752928X16000093

[32] V. Poposka, B. Janeska, A. Gutevska, and A. Duma, "Estimation of time since death through electric and chemical excitability of muscles," *Prilozi/Makedonska Akademija Na Naukite I Umetnostite, Oddelenie Za Biološki I Medicinski Nauki=Contrib./Macedonian Academy Sci. Arts, Sect. Biol. Med. Sci.*, vol. 32, pp. 211–218, Jul. 2011.

[33] B. Knight and K. Simpson, *Simpson's Forensic Medicine*. London, U.K.: E. Arnold, 1997.

[34] P. Saukko and B. Knight, *Knight's Forensic Pathology*, 3rd ed. Boca Raton, FL, USA: CRC Press, 2004.

[35] E. Abraham, M. Cox, and D. Quincey, "Pig-mentation: Postmortem iris color change in the eyes of *Sus scrofa*," *J. Forensic Sci.*, vol. 53, no. 3, pp. 626–631, May 2008. [Online]. Available: https://onlinelibrary.wiley.com/doi/abs/10.1111/j.1556-4029.2008.00729.x

[36] D. Dolinak, E. Matshes, and E. Lew, *Forensic Pathology*, 1st ed. San Diego, CA, USA: Elsevier, 2005.

[37] A. Sansola, "Postmortem iris recognition and its application in human identification," M.S. thesis, School Med., Boston Univ., Boston, MA, USA, 2015.

[38] S. K. Saripalle, A. McLaughlin, R. Krishna, A. Ross, and R. Derakhshani, "Post-mortem iris biometric analysis in sus scrofa domesticus," in *Proc. IEEE 7th Int. Conf. Biometrics Theory, Appl. Syst. (BTAS)*. Arlington, VA, USA: IEEE, Sep. 2015, pp. 1–5.

[39] M. Trokielewicz, A. Czajka, and P. Maciejewicz, "Post-mortem iris decomposition and its dynamics in morgue conditions," 2019, *arXiv:1911.02837*. [Online]. Available: http://arxiv.org/abs/1911.02837

[40] M. Trokielewicz and A. Czajka, "Data-driven segmentation of post-mortem iris images," in *Proc. Int. Workshop Biometrics Forensics (IWBF)*. Sassari, Italy: IEEE, Jun. 2018, pp. 1–7. [Online]. Available: http://arxiv.org/abs/1807.04154

[41] M. Trokielewicz, A. Czajka, and P. Maciejewicz, "Presentation attack detection for cadaver iris," in *Proc. IEEE 9th Int. Conf. Biometrics Theory, Appl. Systems (BTAS)*. Redondo Beach, CA, USA: IEEE, Oct. 2018, pp. 1–10. [Online]. Available: http://arxiv.org/abs/1807.04058

[42] M. Trokielewicz, A. Czajka, and P. Maciejewicz, "Post-mortem iris recognition with Deep-Learning-based image segmentation," 2019, *arXiv:1901.01708*. [Online]. Available: http://arxiv.org/abs/1901.01708

[43] M. Trokielewicz, A. Czajka, and P. Maciejewicz, "Post-mortem iris recognition with deep-learning-based image segmentation," *Image Vis. Comput.*, vol. 94, Feb. 2020, Art. no. 103866, doi: 10.1016/j.imavis.2019.103866.

[44] M. Trokielewicz, "Iris recognition methods resistant to biological changes in the eye," Ph.D. dissertation, Inst. Control Comput. Eng., Warsaw Univ. Technol., Warsaw, Poland, 2019. [Online]. Available: http://zbum.ia.pw.edu.pl/PAPERS/Trokielewicz_PhD_2019.pdf

[45] M. Trokielewicz, A. Czajka, and P. Maciejewicz, "Post-mortem iris recognition resistant to biological eye decay processes," in *Proc. IEEE Winter Conf. Appl. Comput. Vis. (WACV)*. Aspen, CO, USA: IEEE, Mar. 2020, pp. 1–8. [Online]. Available: http://arxiv.org/abs/1912.02512

[46] J. G. Daugman, "High confidence visual recognition of persons by a test of statistical independence," *IEEE Trans. Pattern Anal. Mach. Intell.*, vol. 15, no. 11, pp. 1148–1161, Nov. 1993.

[47] G. W. Quinn, P. Grother, and J. Matey, "IREX IX part one: Performance of Iris recognition algorithms," NIST, Gaithersburg, MD, USA, Interagency Rep. 7629, 2018, doi: 10.6028/NIST.IR.8207.

[48] A. Czajka, D. Moreira, K. Bowyer, and P. Flynn, "Domain-specific human-inspired binarized statistical image features for iris recognition," in *Proc. IEEE Winter Conf. Appl. Comput. Vis. (WACV)*. Waikoloa Village, HI, USA: IEEE, Jan. 2019, pp. 959–967.

[49] M. Trokielewicz, A. Czajka, and P. Maciejewicz, "Perception of image features in post-mortem iris recognition: Humans vs machines," in *Proc. IEEE 10th Int. Conf. Biometrics Theory, Appl. Syst. (BTAS)*. Tampa, FL, USA: IEEE, Sep. 2019, pp. 1–9. [Online]. Available: http://arxiv.org/abs/1807.04049

[50] U-JIN LED. *ULI-81036A-30IRP IR Lamp Specification*. Accessed: Jul. 3, 2020. [Online]. Available: http://ujin.ezion.co.kr/down/ULI-81036A-30IRP.pdf

[51] B. J. Balas and P. Sinha, "STICKS: Image-representation via non-local comparisons," *J. Vis.*, vol. 3, p. 12, Oct. 2003.

[52] K. B. Raja, R. Raghavendra, and C. Busch, "Binarized statistical features for improved iris and periocular recognition in visible spectrum," in *Proc. 2nd Int. Workshop Biometrics Forensics*. Valletta, Malta: IEEE, Mar. 2014, pp. 1–6.

[53] A. Gangwar and A. Joshi, "DeepIrisNet: Deep iris representation with applications in iris recognition and cross-sensor iris recognition," in *Proc. IEEE Int. Conf. Image Process. (ICIP)*. Phoenix, AZ, USA: IEEE, Sep. 2016, pp. 2301–2305.

[54] C. Chen and A. Ross, "A multi-task convolutional neural network for joint iris detection and presentation attack detection," in *Proc. IEEE Winter Appl. Comput. Vis. Workshops (WACVW)*. Lake Tahoe, NV, USA: IEEE, Mar. 2018, pp. 44–51.

[55] E. Jalilian and A. Uhl, "Iris segmentation using fully convolutional encoder–decoder networks," in *Deep Learning for Biometrics*. Salzburg, Austria: Springer, 2017, pp. 133–155.

[56] K. Nguyen, C. Fookes, A. Ross, and S. Sridharan, "Iris recognition with off-the-shelf CNN features: A deep learning perspective," *IEEE Access*, vol. 6, pp. 18848–18855, 2018.

[57] Chinese Academy of Sciences. (2004). *CASIA-Iris-Syn v4*. [Online]. Available: http://biometrics.idealtest.org/dbDetailForUser.do?id=4
[58] A. Ross, K. Nandakumar, and A. Jain, *Handbook Multibiometrics*. New York, NY, USA: Springer, 2006. [Online]. Available: http://www.springer.com/us/book/9780387222967
[59] M. Singh, R. Singh, and A. Ross, "A comprehensive overview of biometric fusion," *Inf. Fusion*, vol. 52, pp. 187–205, Dec. 2019.
[60] S. Shah and A. Ross, "Iris segmentation using geodesic active contours," *IEEE Trans. Inf. Forensics Security*, vol. 4, no. 4, pp. 824–836, Dec. 2009.
[61] Neurotechnology. (2019). *VeriEye SDK v11.1*. [Online]. Available: https://www.neurotechnology.com/verieye.html
[62] N. Othman, B. Dorizzi, and S. Garcia-Salicetti, "OSIRIS: An open source iris recognition software," *Pattern Recognit. Lett.*, vol. 82, pp. 124–131, Oct. 2016, doi: 10.1016/j.patrec.2015.09.002.
[63] C. Rathgeb, A. Uhl, P. Wild, and H. Hofbauer, "Design decisions for an Iris recognition SDK," in *Handbook of Iris Recognition* (Advances in Computer Vision and Pattern Recognition), 2nd ed., K. Bowyer and M. J. Burge, Eds. London, U.K.: Springer, 2016.
[64] A. Boyd, A. Czajka, and K. Bowyer, "Deep learning-based feature extraction in iris recognition: Use existing models, fine-tune or train from scratch?" in *Proc. IEEE Int. Conf. Biometrics, Theory Appl. Syst. (BTAS)*. Tampa, FL, USA: IEEE, Sep. 2019, pp. 1–6.
[65] J. Kannala and E. Rahtu, "BSIF: Binarized statistical image features," in *Proc. 21st Int. Conf. Pattern Recognit. (ICPR)*. Tsukuba, Japan: IEEE, Nov. 2012, pp. 1363–1366.
[66] J. Chen, F. Shen, D. Z. Chen, and P. J. Flynn, "Iris recognition based on human-interpretable features," *IEEE Trans. Inf. Forensics Security*, vol. 11, no. 7, pp. 1476–1485, Jul. 2016.

AIDAN BOYD (Student Member, IEEE) received the B.Eng. (Hons.) degree from the National University of Ireland, Galway, in 2018. He is currently pursuing the Ph.D. degree with the University of Notre Dame. He is currently working as a Research Assistant with the Computer Vision Research Laboratory under the supervision of Prof. K. Bowyer and Prof. A. Czajka. His research interests include the application of modern computer vision techniques to iris biometric technologies and the development of generalized machine learning models to address challenges in iris biometrics.

SHIVANGI YADAV received the B.S. and M.S. degrees in computer science and engineering from the Indraprastha Institute of Information Technology, Delhi, India, in 2015 and 2016, respectively. She is currently pursuing the Ph.D. degree in computer science and engineering with Michigan State University, MI, USA. She was a Research Associate with the Indraprastha Institute of Information Technology, from 2016 to 2017. Her research interests include the development of generalized presentation attack detection algorithm for different biometric modalities and also study of deep fakes and synthetic biometric data.

THOMAS SWEARINGEN (Student Member, IEEE) received the B.S. degree in computer engineering from The University of Tennessee, Knoxville, in 2013, and the M.S. degree in computer science from Michigan State University, in 2017, where he is currently pursuing the Ph.D. degree in computer science with the iPRoBe Laboratory, under the supervision of Dr. A. Ross. Prior to joining Michigan State University, he was a Research Intern with the Oak Ridge National Laboratory. His research interests include face recognition, deep learning, and computer vision. He received the Graduate Research Fellowship from the U.S. National Institute of Justice, in 2015.

ANDREY KUEHLKAMP (Member, IEEE) was born in Videira, SC, Brazil, in 1979. He received the B.S. degree in computer science from the University of West Santa Catarina, in 2001, the M.S. degree in applied computing from the University of the Itajai Valley, in 2013, and the Ph.D. degree in computer science and engineering from the University of Notre Dame, in 2018. He has worked as a Software Engineer, from 2001 to 2009, developing corporate distributed systems. From 2005 to 2014, he was a Lecturer Professor in computer science with the University of West Santa Catarina, where he was also a Coordinator of Undergraduate Studies for computer science. In 2014, he has worked as a Research Assistant with the Computer Vision Research Laboratory, University of Notre Dame. Since 2018, he has been a Postdoctoral Research Associate with the Center for Research Computing. He has published over 15 research articles in peer-reviewed and respectable journals and conferences in the field. His research interest includes the intersection between machine learning, biometrics, and distributed systems.

MATEUSZ TROKIELEWICZ (Member, IEEE) received the B.Sc. degree in biomedical engineering from the Faculty of Mechatronics, Warsaw University of Technology, the M.Sc. degree in biomedical engineering from the Faculty of Electronics and Information Technology, Warsaw University of Technology, and the Ph.D. degree (Hons.) in computer science from the Faculty of Electronics and Information Technology, in 2019. Since 2013, he has been with the Biometrics and Machine Intelligence Laboratory, Research and Academic Computer Network NASK. Since 2019, he has been an Assistant Professor with NASK, where he took the lead of the Biometric Systems Group. He has authored or coauthored more than 25 peer-reviewed publications, including papers accepted for the top international conferences and journals related to biometrics and computer vision. His research interests include novel methods and applications of iris biometrics, such as post-mortem iris identification, which he investigates as a part of the International Research Team together with scientists from the University of Notre Dame, USA, and the Medical University of Warsaw. He was a winner of the 2016 EAB European Biometrics Research Award.

ERIC BENJAMIN was a U.S. Marine, from 1977 to 1981, and a Paramedic, from 1981 to 2003. He has been working in forensics, since 1982. He has studied at the Daniel Freedman Hospital for Paramedic Studies before attending the Los Angeles Sheriff's Academy for forensics training in Los Angeles. He has worked for the LA Coroner's Office as a Field Investigator and a Forensic Technician. He then worked with the LAFD as a Paramedic while assigned with a private ambulance service. He has also operated as a Paramedic with the Hyde Park Training Association as the Lead Paramedic and a Medical Legal Investigator for the Dutchess County Medical Examiner. He currently works as a Forensic Autopsy Technician for the Dutchess County Medical Examiner.

PIOTR MACIEJEWICZ received the M.D. and Ph.D. degrees from the Medical University of Warsaw, Poland. He completed his residency at the Ophthalmological Clinic in Warsaw, where he is currently a Medical Staff Member. He is also a General Ophthalmologist with clinical interests focused on early diagnosis of glaucoma and anterior eye segment problems. He is a Laser Photocoagulation Expert in the diabetic retinopathy treatment. He has participated in numerous clinical trials investigating new treatments for retinal diseases, such as neovascular age-related macular degeneration involving novel therapeutic agents. He has been elected to prestigious professional organizations, including the Polish Ophthalmology Society.

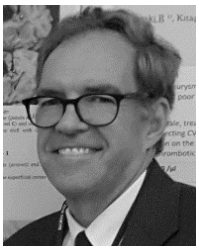

DENNIS CHUTE received the Bachelor of Science degree from the University of Notre Dame, in 1980, and the Medical degree from the Hahnemann Medical School, Drexel University Medical School, in 1985. He completed a residency in Anatomic and Clinical Pathology with the Danbury Hospital, in 1989, and a fellowship in Forensic Pathology at the Office of the Chief Medical Examiner for the State of Maryland, Baltimore, in 1990. He was employed as an Assistant Medical Examiner for the State of Maryland, for ten years, before doing a fellowship in Neuropathology at UCLA after which he worked for two years as an Assistant Professor with the Division of Neuropathology, The David Geffen School of Medicine, UCLA. In 2005, he became the Deputy Medical Examiner for Dutchess County and, then, became the Chief Medical Examiner, in 2014. His research interests include forensic and forensic neuropathology.

ARUN ROSS (Senior Member, IEEE) received the B.E. degree (Hons.) in computer science from BITS Pilani, India, and the M.S. and Ph.D. degrees in computer science and engineering from Michigan State University, USA. He is currently the Cillag Endowed Chair of Science and Engineering, and a Professor with the Department of Computer Science and Engineering, Michigan State University. He has coauthored the textbook, *Introduction to Biometrics* and the monograph, *Handbook of Multibiometrics*. He was a recipient of the NSF CAREER Award and was designated as a Kavli Fellow by the U.S. National Academy of Sciences, in 2006. He received the J. K. Aggarwal Prize, in 2014, and the Young Biometrics Investigator Award, in 2013, from the International Association of Pattern Recognition.

PATRICK FLYNN (Fellow, IEEE) received the Ph.D. degree in computer science from Michigan State University, in 1990. He is currently the Fritz Duda Family Professor of engineering and the Chair of the Department of Computer Science and Engineering, University of Notre Dame. His research interests include computer vision, biometrics, and image processing. He is an IAPR Fellow and an ACM Distinguished Scientist. He has received the Meritorious Service Award, the Golden Core Award, the Certificate of Achievement Award, and the Technical Achievement Award from the IEEE Computer Society.

KEVIN BOWYER (Fellow, IEEE) is currently the Schubmehl-Prein Family Professor of computer science and engineering with the University of Notre Dame. He also serves as the Director of International Summer Engineering Programs for the Notre Dame College of Engineering. In 2019, he was elected as a Fellow of the American Association for the Advancement of Science. He is also a Fellow of the IAPR. He received the Technical Achievement Award from the IEEE Computer Society, with the citation for pioneering contributions to the science and engineering of biometrics. He has served as the Editor-in-Chief for the IEEE TRANSACTIONS ON PATTERN ANALYSIS AND MACHINE INTELLIGENCE. He currently serves as the Editor-in-Chief for the IEEE TRANSACTIONS ON BIOMETRICS, BEHAVIOR, AND IDENTITY SCIENCE.

ADAM CZAJKA (Senior Member, IEEE) is currently an Assistant Professor with the Department of Computer Science and Engineering, College of Engineering, University of Notre Dame. He is the VP for Finance of the IEEE Biometrics Council. Before coming to Notre Dame, he was the Chair of the Biometrics and Machine Learning Laboratory, Institute of Control and Computation Engineering, WUT, the Head of the Postgraduate Studies on Security and Biometrics, the Vice Chair of the NASK Biometrics Laboratory, the Chair of the Polish Standardization Committee on Biometrics, an Assistant Professor with NASK–National Research Institute in Poland, and a member of the NASK Research Council.